

THERMAL DISPLACEMENTS IN COPPER-GOLD ALLOYS

by
Charles Matthew Gilmore

//

Dissertation submitted to the Faculty of the Graduate School
of the University of Maryland in partial fulfillment
of the requirements for the degree of
Doctor of Philosophy
1971

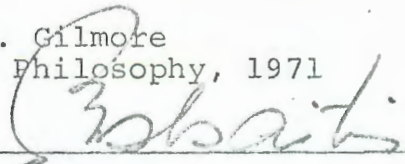
copy!

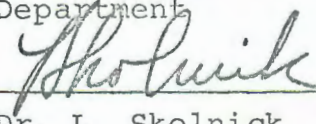
APPROVAL SHEET

Title of Thesis: Thermal Displacements in Copper-Gold Alloys

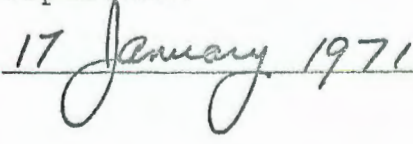
Name of Candidate: Charles M. Gilmore
Doctor of Philosophy, 1971

Thesis and Abstract Approved:


Dr. P. Bolsaitis
Associate Professor
Engineering Materials Group of
the Chemical Engineering
Department


Dr. L. Skolnick
Professor
Engineering Materials Group of
the Chemical Engineering
Department

Date Approved:


17 January 1971

ABSTRACT

Title of Thesis: Thermal Displacements in Copper-Gold Alloys

Charles M. Gilmore, Doctor of Philosophy, 1971

Thesis directed by: Dr. P. Bolsaitis
Associate Professor

Dr. L. Skolnick
Professor

The thermal displacements and Debye temperatures are determined for single crystals of copper and Cu-Au solid solutions including Cu_3Au of four degrees of long range order (0.0, 0.53, 0.8, .98). Other solid solution compositions studied were .91Cu-.09Au and .2Cu-.8Au. At the .91Cu-.09Au composition a one week anneal produced a nonequilibrium structure. After a one month anneal the thermal displacements decreased to a value nearly equal to the value for pure Cu. The thermal displacements in the quenched .75Cu-.25Au crystal were also nearly equal to the value for pure Cu, but the thermal displacements increased as the Cu_3Au crystal approached the equilibrium condition of full order.

In the Cu_3Au crystals, which were partially or fully ordered, the thermal displacements of the individual Cu and Au atoms were determined. It was observed that the vibration amplitudes of the Cu atoms are not isotropic in this diatomic cubic crystal. The vibrations of the Au atoms are equal in the [110] and [001] directions within experimental uncertainty. Also, the thermal displacements decrease as

the crystal is changed from fully ordered to fully disordered. This is consistent with calculations of the vibrational spectrum for ordered and disordered Cu_3Au . The static displacements for the partially ordered $S = .80$ crystal were also determined from the same experiments as the thermal displacements.

An Einstein model was developed to calculate thermal displacements and Einstein frequencies from interatomic potentials. The calculated thermal displacements are 10 to 20 percent less than the experimental values. This is due to the simplifying assumptions in the model. The model calculation and the experimental results do agree on the changes in the thermal displacements with alloying. The Einstein model is also used to calculate the vibrational entropy in alloys.

DEDICATION

This work is dedicated to the memory of my parents
Charles Matthew and Ruth Elizabeth Gilmore.

ACKNOWLEDGMENTS

Few things of any magnitude are ever accomplished by a lone person. Success depends upon the proper conditions and the proper people being present at the same time. There were many who were present during the progress of this work that made it possible.

First, I thank Dr. Pedro Bolsaitis for creating the atmosphere where I could develop as a scientist and a person. He was always available with learned advice and guidance when I was in need of direction. Equally important was his patience and encouragement as I wrestled with new problems and his understanding and confidence in my solutions. It is under these conditions that creative and original work has the best chance to develop.

This project originated out of the interest of Dr. Leonard Skolnick. It was Dr. Skolnick's enthusiasm that originally brought me to the Engineering Materials Group. The work of Dr. Skolnick and Dr. J. Marchello in establishing the Engineering Materials Group may affect my life more than any other event, my gratitude cannot be adequately expressed. Also, because of Dr. Skolnick's efforts the X-ray laboratory and the costly equipment were available.

The assistance and guidance provided by Dr. Earl Skelton, Dr. Barry Klein and Dr. Joseph Feldman of the Naval Research Laboratory are gratefully acknowledged.

They were all patient and understanding as I sought to understand the difficult concepts which they have mastered. I would also like to thank Mr. David Nagel of the Naval Research Laboratory for many stimulating discussions.

There were many people at the University of Maryland who advised me on my experiments and who graciously allowed me to use their equipment. In particular I would like to note the contributions of Dr. Ian Spain, Dr. R. J. Arsenault and Dr. S. M. Bhagat.

The assistance provided by Mr. Anthony Verbalis in the final stages of this research is gratefully acknowledged; his enthusiasm and hard work provided significant progress in this project. The contributions of Mr. Roger Chiarodo, who provided the crystals for this study and elastic constant data, helped to make this project a more complete and relevant study.

Special acknowledgment is due to my wife Charlotte for her many years of patience, encouragement, deprivation, and understanding during my graduate studies. Her assistance in typing the initial drafts of this thesis was of invaluable assistance. I finally thank Mrs. Peggy Hood whose masterful typing made this thesis appear in its final form.

TABLE OF CONTENTS

Chapter	Page
DEDICATION.....	ii
ACKNOWLEDGMENTS.....	iii
I. INTRODUCTION.....	1
1.1 Thesis objectives.....	1
1.2 Background.....	5
1.3 Thermal displacements in disordered Cu-Au alloys.....	19
1.4 Thermal displacements in ordered Cu ₃ Au alloys.....	23
II. EXPERIMENTS.....	26
2.1 Introduction.....	26
2.2 Specimen preparation and analysis.....	26
2.3 Equipment.....	27
2.4 Determination of lattice parameter, composition and homogeneity.....	30
2.5 Determination of long range order parameter in Cu ₃ Au alloys.....	40
2.6 Introduction to measurement of thermal displacements of Cu-Au alloys.....	42
2.7 Experimental techniques for the mea- surement of thermal displacements by the two temperature method.....	46
2.8 Determination of thermal displacements by Flinn's technique.....	53

Chapter	Page
2.9 Determination of thermal displacements in partially ordered Cu_3Au	56
2.10 Determination of thermal displacements in ordered Cu_3Au crystals by the one temperature technique.....	59
2.11 Separation of thermal displacements of constituent atoms in disordered alloys	62
2.12 Summary of experiments to measure thermal displacements.....	66
III. RESULTS AND DISCUSSION.....	67
3.1 Disordered Cu-Au alloys.....	67
3.2 Cu_3Au crystals.....	70
IV. APPLICATION OF EXPERIMENTAL RESULTS TO CELLULAR ALLOY MODEL.....	82
4.1 Background.....	82
4.2 Model calculation of thermal dis- placements.....	84
V. CONCLUSIONS.....	94
APPENDIX A. THERMAL DIFFUSE SCATTERING CORRECTION	97
APPENDIX B. COMPUTER PROGRAM FOR DETERMINATION OF THERMAL DISPLACEMENTS BY THE TWO TEMPERATURE TECHNIQUE AT ROOM AND LIQUID NITROGEN TEMPERATURES.....	106
APPENDIX C. COMPUTER PROGRAM TO DETERMINE THERMAL DISPLACEMENTS BY FLINN'S TECHNIQUE....	112

Chapter	Page
APPENDIX D. COMPUTER PROGRAM TO CORRECT INTEGRATED INTENSITIES FOR THERMAL DIFFUSE SCATTER.....	117
APPENDIX E. SAMPLE DATA OUTPUT.....	119
SELECTED BIBLIOGRAPHY.....	121

LIST OF TABLES

Table		Page
1.1	DEBYE TEMPERATURES AND THERMAL DISPLACEMENTS FOR DISORDERED Cu-Au ALLOYS AT 298°K.....	20
1.2	ROOM TEMPERATURE THERMAL DISPLACEMENTS IN Cu ₃ Au CRYSTALS.....	24
2.1	ANNEALING SCHEDULE OF THE Cu-Au ALLOYS COMPOSITION IN ATOMIC PERCENT.....	28
2.2	X-RAY ANALYSIS OF Cu-Au ALLOYS.....	38
2.3	EXPERIMENTAL VALUES FOR THE DETERMINATION OF <i>S</i>	41
2.4	RESISTANCES (<i>R</i> ₂) IN TEMPERATURE SENSING CIRCUIT.....	50
3.1	EXPERIMENTAL R.M.S. THERMAL DISPLACEMENTS IN DISORDERED Cu-Au ALLOYS.....	68
3.2	EXPERIMENTAL R.M.S. THERMAL DISPLACEMENTS FOR Cu ₃ Au DETERMINED FROM (400) REFLECTIONS AS A FUNCTION OF THE LONG RANGE ORDER PARAMETER (<i>S</i>).....	71
3.3	EXPERIMENTAL R.M.S. THERMAL DISPLACEMENTS OF Cu AND Au ATOMS IN Cu ₃ Au AS A FUNCTION OF THE DEGREE OF LONG RANGE ORDER (<i>S</i>).....	73
3.4	MEASUREMENTS OF R.M.S. THERMAL DISPLACEMENTS FOR Cu and Au ATOMS IN Cu ₃ Au.....	74
3.5	DEBYE TEMPERATURES FOR ORDERED AND DISORDERED Cu ₃ Au CRYSTALS.....	79
3.6	R.M.S. TOTAL DISPLACEMENTS IN PARTIALLY ORDERED Cu ₃ Au CRYSTALS.....	81
3.7	R.M.S. STATIC DISPLACEMENTS IN PARTIALLY ORDERED Cu ₃ Au CRYSTALS.....	81

Table		Page
4.1	PARAMETERS FOR CELL MODEL POTENTIAL.....	86
4.2	INTERATOMIC DISTANCES FROM CELL MODEL....	87
4.3	COMPARISON OF R.M.S. THERMAL DISPLACEMENTS CALCULATED WITH BORN-V.KARMAN AND EINSTEIN MODELS AT 298°K.....	88
4.4	EXPERIMENTAL THERMAL DISPLACEMENTS AND LATTICE PARAMETERS; CALCULATED THERMAL DISPLACEMENTS, EINSTEIN FREQUENCIES AND VIBRATIONAL ENTROPIES FOR DISORDERED Cu-Au ALLOYS.....	93
A.1	ELASTIC CONSTANTS FOR Cu-Au CRYSTALS IN 10^{12} DYNES/CM ²	99

LIST OF FIGURES

Figures		Page
1.1	SCHEMATIC OF DIFFRACTION CONDITIONS...	7
1.2	SCHEMATIC OF LATTICE.....	7
2.1	SCHEMATIC OF X-RAY DIFFRACTION EXPERIMENT.....	29
2.2	DEGREES OF FREEDOM FOR THE SAMPLE.....	32
2.3	LATTICE PARAMETER IN kx FOR Cu-Au ALLOYS.....	39
2.4	SCHEMATIC OF CRYOSTAT.....	47
2.5	TEMPERATURE SENSING CIRCUIT.....	49
3.1	X-RAY DIFFRACTION DATA FOR Cu_3Au , S = .98, [110] DIRECTION.....	72
3.2	X-RAY DIFFRACTION DATA FOR Cu_3Au , S = .98, [001] DIRECTION.....	76
4.1	TWO DIMENSIONAL SCHEMATIC OF AN EINSTEIN CELL.....	90

LIST OF SYMBOLS

M	-	Debye-Waller factor
M_f	-	Debye-Waller factor for a fundamental reflection
M_s	-	Debye-Waller factor for a superlattice reflection
I	-	Integrated Bragg intensity
$\overline{U_s^2}$	-	Mean square vibration amplitude in the s direction
θ	-	Bragg diffraction angle
λ	-	Wave length of diffracted radiation
S_{vib}	-	Vibrational entropy
N	-	Number of unit cells in the lattice
k	-	Boltzman's constant
h	-	Planck's constant
\hbar	-	$h/2\pi$
ν_E	-	Einstein frequency
ν_M	-	X-ray Debye frequency
T	-	Temperature
m	-	Atomic weight
E	-	Energy
θ	-	General Debye temperature
θ_M	-	X-ray Debye temperature
θ_T	-	Melting point Debye temperature
θ_D	-	Specific heat Debye temperature
θ_E	-	Elastic constant Debye temperature
θ_R	-	Electrical resistivity Debye temperature

- ρ - Material density
- ν - Circular frequency of phonon waves
- ω - Angular frequency of phonon waves
- \bar{k} - Wave vector for radiation
- q - Phonon wave vector
- FC - Atomic force constant
- d_{hkl} - Interplanar spacing
- a - Lattice parameter
- S - Long range order parameter
- L_p - Lorentz polarization factor
- α - Linear expansion coefficient
- γ - Grüneisen constant
- Ω - Crystal rotation angle about the Z axis
- χ - Crystal rotation angle about the Y axis
- f - Atomic scattering factor
- F - Structure factor
- x - Concentration
- Δ - Imaginary component of anomalous scattering factor
- $\Delta f'$ - Real component of anomalous scattering factor
- K - Scattering vector

CHAPTER I

INTRODUCTION

1.1 Thesis objectives

The objective of the experimental portion of this thesis was to measure the atomic root mean square (R.M.S.) thermal vibration amplitudes and Debye temperatures in copper-gold alloys. This was done for disordered alloys of three different compositions and for various degrees of order for the Cu_3Au composition. The measurements were made using several X-ray diffraction techniques to be described in the text. The techniques all result in a measurement of the Debye-Waller factor (M) for a Bragg reflection. The results of the theory initially worked out by Debye (1914) and then corrected by Waller (1923) can be summarized in an equation of the form

$$I = I_0 \exp(-2M) \quad . \quad [1.1]$$

I is the diffracted intensity for the crystal with vibrating atoms and I_0 is the intensity if the atoms are at rest. The value of M can be used to evaluate the mean square thermal vibration amplitude ($\overline{U_s^2}$) in the direction s by the relation

$$M = 8\pi^2 \overline{U_s^2} \left(\frac{\sin \theta}{\lambda} \right)^2 \quad . \quad [1.2]$$

There are several reasons for studying the thermal displacements in solids which will be discussed in the following paragraphs. First, the thermal displacements

provide fundamental information about the forces between atoms in solids. As will be discussed in Chapter IV, the thermal displacements at high temperatures can be related to the interatomic force constants. When combined with lattice models such as those of Einstein or Debye, the thermal displacements can be utilized to determine or to test interatomic force constants. Thus, the thermal displacements will reveal how the interatomic forces are changing with alloying and with changes in degree of order. This is one of the immediate uses of the data from this experimental program. The measured thermal displacements will be compared with those calculated from an Einstein model of the alloy. The interatomic potentials were obtained from a cellular model for alloys developed by Bolsaitis and Skolnick (1968). This subject will be discussed in more detail later in the text.

The data on the thermal displacements was also used to calculate the vibrational entropy in Cu-Au alloys. In the alloy model proposed by Bolsaitis and Skolnick, certain parameters must be determined by a minimization of the Gibbs free energy. The vibrational entropy (S_{vib}) can be calculated in the Einstein approximation from the relation

$$S_{vib} = -3Nk \left\{ \ln \left[1 - \exp\left(-\frac{h\nu_E}{kT}\right) \right] - \frac{h\nu_E/kT}{\exp\left(-\frac{h\nu_E}{kT}\right) - 1} \right\}, \quad [1.3]$$

which was presented by Born and Huang (1955), where ν_E is the Einstein frequency. The Einstein frequency was calculated with potentials derived from the cell model

and these results will be checked by experiment. Experimental values of ν_E can be obtained from the Debye frequency (ν_M) as discussed by Blackman (1937) where the relationship

$$\nu_E = \frac{1}{\sqrt{3}} \nu_M \quad [1.4]$$

was derived. The Debye frequency is obtained directly from the Debye temperature θ_M through the equation

$$h\nu_M = k\theta_M \quad [1.5]$$

Equally important data can come from the thermal displacements by applying the Debye lattice theory. The X-ray Debye temperature (θ_M) can be determined from the thermal displacements through the relation

$$\theta_M^2 = \frac{3 h^2 T}{4\pi^2 m k \bar{U}_s^2} \left\{ \phi\left(\frac{\theta_M}{T}\right) + \frac{\theta_M}{4T} \right\} ; \quad [1.6]$$

where $\phi\left(\frac{\theta_M}{T}\right)$ is defined in equation [1.56] of this text.

θ_M is a parameter which can be utilized in calculating many thermodynamic properties of solids which have not been previously investigated. θ_M is of value because thermodynamic properties can be calculated by integrations over the frequency spectrum. Thus macroscopic properties are not dependent on the fine structure of the spectrum, but only upon the integral over the spectrum. As shown by Blackman (1955), the Debye-Waller factor (M) is an inverse second moment of the vibration energy (ν_{vib}) over the frequency spectrum:

$$M = \frac{2 \sin^2 \theta}{3\lambda^2 N_m} \sum_v \frac{E(\nu)}{\nu^2} , \quad [1.7]$$

where ν is the vibration frequency of the q th mode, N is the number of unit cells in the lattice, θ is the Bragg diffraction angle, λ the X-ray wave length, and m is the atomic mass. If we substitute a Debye spectrum for the real spectrum, a maximum frequency ν_M can be chosen that will give the same inverse second moment as the real spectrum. The X-ray Debye temperature is then given by

$$h\nu_M = k\theta_M . \quad [1.8]$$

The value of θ_M can be used to calculate other properties at the same temperature which are dependent upon the inverse second moment of the frequency distribution.

A little care must be exercised in applying the X-ray Debye temperature to the solution of problems. The Debye temperature is not independent of temperature, thus the value for θ_M determined at room temperature must be corrected to be applied at other temperatures. Also, care must be exercised in using θ_M to calculate other properties which depend upon the frequency distribution in a different manner than the Debye-Waller factor. Blackman (1955) has discussed the dependence of thermodynamic properties on different moments over the frequency spectrum.

Provided one is aware of these limitations on the application of X-ray Debye temperatures, the value of θ_M can be used to obtain approximate information on many properties related to the Debye temperature. Blackman (1955) has reviewed some of these relationships. The compressibility C has been related to a Debye temperature by Einstein (1911):

$$\theta_x = A C^{-1/2} m^{-1/3} \rho^{-1/6} \quad [1.9]$$

where A is a material constant, m is the atomic or molecular weight, and ρ is the density. Lindeman (1910) has defined a Debye temperature in terms of the melting point (T_M) of the solid:

$$\theta_T = B \left(\frac{T_M}{mV^{2/3}} \right)^{1/2} \quad [1.10]$$

where B is another material constant, and V is the mean atomic volume. The Debye temperature can also be used to calculate the specific heat at constant volume C_v :

$$C_v = 9Nk \left(\frac{T}{\theta} \right)^3 \int_0^{z_D} \frac{e^z z^4 dz}{(e^z - 1)^2} \quad [1.11]$$

where $z = \hbar\omega/kT$ and $z_D = \theta/T$. Kittel (1953) shows how the conductivity (σ) at high temperatures can be calculated from the Debye temperature:

$$\sigma = \frac{e^2 m k \theta^2}{2 P^3 \bar{Q}_s T} \quad [1.12]$$

where P is the electronic momentum, and \bar{Q}_s is the free space scattering cross section of an atom for an electron. This is only a partial list of the thermodynamic properties that can be related to the Debye temperature. The point is that values of Debye temperatures can be used in many studies of solids to calculate uninvestigated properties.

1.2 Background

The use of a Debye lattice model to obtain expressions for the Debye-Waller factor in terms of Debye temperatures

and thermal displacements is a central part of this study. Therefore, it is necessary to derive the Debye-Waller factor for Bragg diffraction of X-rays from fundamental principles to see what approximations are necessary to obtain the final equations. This will also demonstrate the substitution of a Debye spectrum with a cutoff at frequency ω_M for the real spectrum. This is a valuable concept in the treatment of the thermodynamics of alloys.

This development is primarily taken from Ziman (1964). The diffraction process can be considered to be a scattering of the incident radiation of wave vector \vec{k} to a wave vector of \vec{k}' as shown in Figure 1.1. In the Born approximation of perturbation theory the rate of scattering from the initial state of $\psi_{\vec{k}}$ to the final state of $\psi_{\vec{k}'}$ by a potential $V(r)$ at r is given by the matrix element

$$M_{\vec{k}', \vec{k}} = \int \psi_{\vec{k}'}^*(r) V(r) \psi_{\vec{k}}(r) dv . \quad [1.13]$$

For X-rays the states $\psi_{\vec{k}}(r)$ are plane wave states:

$$\psi_{\vec{k}}(r) = \exp(i\vec{k} \cdot r) , \quad [1.14]$$

and the potential for scattering X-rays is the electron density $\rho(r)$. $\rho(r)$ for a crystal lattice with thermal vibrations is a sum over the L lattice sites of the atomic electron density ρ_a :

$$\rho(r) = \sum_L \rho_a (r - R_L) , \quad [1.15]$$

where R_L is the position of an atom at the lattice site L .

Thus, the scattering matrix can be rewritten as

$$M_{\vec{k}', \vec{k}} = \int e^{-i\vec{k}' \cdot r} \sum_L \rho_a (r - R_L) e^{i\vec{k} \cdot r} dv . \quad [1.16]$$

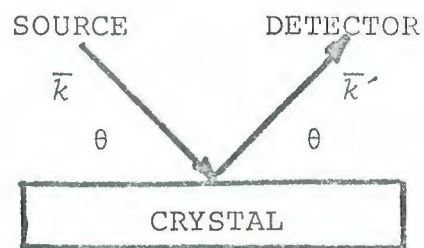


FIGURE 1.1 SCHEMATIC OF DIFFRACTION CONDITIONS

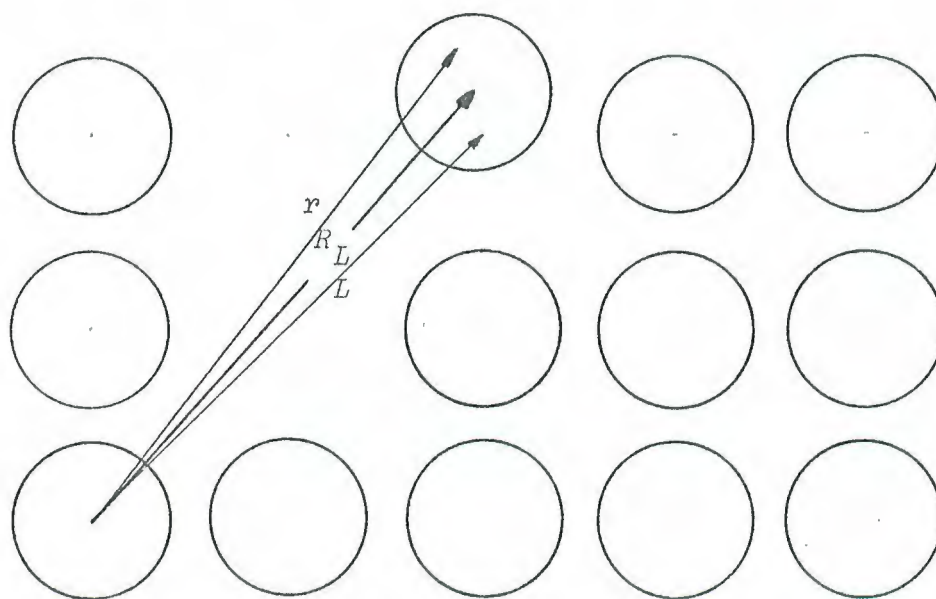


FIGURE 1.2 SCHEMATIC OF LATTICE

Multiplying by $e^{i(\bar{k}-\bar{k}')\cdot R_L}$ and $e^{-i(\bar{k}-\bar{k}')\cdot R_L}$ and rearranging terms results in

$$M_{\bar{k}', \bar{k}} = \sum_L e^{-i(\bar{k}-\bar{k}')\cdot R_L} \int e^{i(\bar{k}-\bar{k}')\cdot (r-R_L)} \rho_a(r-R_L) dv. \quad [1.17]$$

Now introducing the scattering vector

$$K = \bar{k}' - \bar{k}, \quad [1.18]$$

the scattering matrix can be written as

$$M_{\bar{k}', \bar{k}} = \sum_L e^{-iK\cdot R_L} \int \rho_a(r_a) e^{-iK\cdot r_a} dv, \quad [1.19]$$

where r_a is defined as the distance from the atom's center.

The atomic factor $f(K)$ is defined as the Fourier transform of the atomic electron density:

$$f(K) = \int \rho_a(r) e^{-i(K\cdot r)} dv, \quad [1.20]$$

and the structure factor SF as

$$SF = \sum_L e^{-iK\cdot R_L}. \quad [1.21]$$

Consider each atom at a lattice site L to be displaced by U_L so that

$$R_L = L + U_L. \quad [1.22]$$

The displacement U_L for one polarization is the sum of displacements U_q of wave vector q :

$$U_L = \sum_q U_q e^{iq\cdot L}. \quad [1.23]$$

Substituting R_L into the structure factor results in

$$\sum_L e^{-iK \cdot R_L} = \sum_L e^{-iK \cdot L} \prod_q e^{-iK \cdot U_q} e^{iq \cdot L} . \quad [1.24]$$

Expanding the part of the structure factor which is summed over q yields

$$e^{-iK \cdot U_q} e^{iq \cdot L} = 1 - iK \cdot U_q e^{iq \cdot L} - \frac{1}{2} |K \cdot U_q|^2 . \quad [1.25]$$

If there were no coupling between the atomic displacements the second term would average to zero. But due to the coupling between atomic displacements, as in the Born-v.Karman model of a lattice, this term results in thermal diffuse scatter. Because this term averages to a small value in comparison to the squared term it will be dropped for now even though it will be considered as a correction to the final data. Thus the structure factor can be written as

$$\sum_L e^{-iK \cdot R_L} \approx \sum_L e^{-iK \cdot L} \prod_q \left(1 - \frac{1}{2} |K \cdot U_q|^2 \right) , \quad [1.26]$$

where the term $\sum_L e^{-iK \cdot L}$ is just the standard structure factor which determines where the Bragg reflections occur. The remainder of the structure factor can be written as

$$\prod_q \left(1 - \frac{1}{2} |K \cdot U_q|^2 \right) = e^{-M_L} , \quad [1.27]$$

where M_L is the Debye-Waller factor of the atom at the L

lattice site. Using the algebraic expansion:

$$\lim_{N \rightarrow \infty} \prod_1^N \left(1 - \frac{1}{N} a_n\right) = \exp \left\{ -\lim_{N \rightarrow \infty} \frac{1}{N} \sum_{n=1}^N a_n \right\} \quad [1.28]$$

equation [1.27] can be written as

$$\prod_q \left(1 - \frac{1}{2} |K \cdot U_q|^2\right) = \exp \left\{ -\frac{1}{2} \sum_q |K \cdot U_q|^2 \right\}. \quad [1.29]$$

The Debye-Waller factor (M_L) can now be written as

$$M_L = \frac{1}{2} \sum_q |K \cdot U_q|^2. \quad [1.30]$$

To evaluate the Debye-Waller factor the amplitude of vibration must be expressed in terms of the vibrational energy. The Virial Theorem states that for a harmonic oscillator the total energy (\bar{E}) is equal to twice the average kinetic energy and that the average kinetic energy is equal to the average potential energy. Thus, we can write for one polarization

$$\begin{aligned} \bar{E} &= N m |\dot{U}|^2 \\ &= N \sum_q m |\dot{U}_q|^2 \\ &= N \sum_q m \omega_q^2 |U_q|^2, \end{aligned} \quad [1.31]$$

where ω_q is the angular frequency of the q th mode. In the last step the average kinetic and potential energy were equated to give

$$|\dot{U}_q|^2 = \frac{FC}{m} |U_q|^2 = \omega_q^2 |U_q|^2, \quad [1.32]$$

where FC is the atomic force constant.

If we consider only the lattice vibrations in the direction K , the Debye-Waller factor can be written as

$$M_L = \frac{1}{2N} \sum_q K^2 \left(\frac{E_q}{m\omega_q^2} \right) . \quad [1.33]$$

As can be seen in equation [1.33], the Debye-Waller factor is a sum over the real frequency distribution. The value of M_L thus is dependent on the result of the sum, and if we substituted an artificial distribution for the real one which gave the same sum the Debye-Waller factor would be unchanged. A Debye spectrum will be substituted for the real spectrum, and the Debye spectrum of vibration frequencies will be summed to the limiting maximum frequency giving the proper value of M_L . Then the frequency distribution will be cut off at ω_M which is called the Debye frequency, which can be related to the X-ray Debye temperature (θ_M) through

$$\hbar\omega_M = k\theta_M . \quad [1.34]$$

The Debye frequency thus tells us now much of the Debye spectrum is necessary to give the same inverse second moment as the real spectrum.

The Debye-Waller factor will now be developed within the formalism of the Debye model. For any one polarization on the average

$$|K \cdot U_q|^2 = \frac{1}{3} K^2 |U_q|^2 , \quad [1.35]$$

but upon summing the three polarization directions the

result is:

$$|K \cdot U_q|^2 = K^2 |U_q|^2 \quad [1.36]$$

For Bragg diffraction the scattering vector K is given by

$$K = \frac{2\pi}{d_{hkl}} \quad [1.37]$$

where d_{hkl} is the interplanar distance between the planes (hkl) . Using Bragg's law:

$$\lambda = 2d_{hkl} \sin \theta \quad [1.38]$$

the scattering vector is

$$K = 4\pi \frac{\sin \theta}{\lambda} \quad [1.39]$$

Substituting equations [1.36] and [1.39] into equation [1.30] a relation of the form

$$M_L = 8\pi^2 \sum_q |M_q|^2 \sin^2 \theta / \lambda^2 = 8\pi^2 |\overline{U_K}|^2 \sin^2 \theta / \lambda^2 \quad [1.40]$$

is obtained, $\overline{U_K}^2$ is the mean square thermal displacement in the K direction.

To continue to analyze the Debye-Waller factor requires a knowledge of the lattice spectrum in the Debye model. To determine this the following assumptions are made:

1. Only acoustic modes are considered, and there is no dispersion i.e. all modes have the same velocity (S):

$$S = \omega_q / q \quad [1.41]$$

2. The Brillouin zone which limits the values of q is replaced by a Debye sphere of equal volume

in reciprocal space. The radius of the Debye sphere q_M limits the values of q .

An important theorem of solids is that the Brillouin zone contains N points where N is the number of unit cells in the crystal. These N points are uniformly distributed throughout reciprocal space. Therefore, $D(\omega)d\omega$ the fraction of modes from frequency ω to $\omega+d\omega$, which is the same as the fraction of volume from q to $q+dq$, is given by

$$D(\omega)d\omega = \frac{4\pi q^2 dq}{\frac{4}{3}\pi q_M^3} \quad [1.42]$$

From assumption number one above we obtain the Debye spectrum

$$D(\omega)d\omega = \frac{4\pi\omega^2 d\omega}{\frac{4}{3}\pi\omega_M^3} = \frac{3\omega^2}{\omega_D^3} d\omega \quad [1.43]$$

Returning now to an evaluation of the Debye-Waller factor in equation [1.33], the average energy of the q th mode of a quantum oscillator can be expressed as

$$E_q = (\bar{n}_q + \frac{1}{2}) \hbar\omega_q \quad [1.44]$$

where \bar{n}_q , the average number of phonons in mode q , is given according to Bose-Einstein statistics by

$$\bar{n}_q = \frac{1}{e^{\hbar\omega_q/kT} - 1} \quad [1.45]$$

M_L can now be written as

$$M_L = \frac{K^2 \hbar}{2mN} \sum_q \frac{(\bar{n}_q + \frac{1}{2})}{\omega_q} \quad [1.46]$$

The Debye model will now be used to evaluate the sum over the number of modes. The number of modes can be determined by integrating over the volume in reciprocal space

and multiplying by the density of modes in reciprocal space. The density of modes is given by the number of modes in the zone N divided by the volume of the zone $8\pi^3/a^3$ where a^3 is the volume of the zone, i.e.

$$\text{Density} = \frac{N a^3}{8\pi^3} = \frac{V}{8\pi^3} \quad . \quad [1.47]$$

The crystal will be chosen to have a unit volume and the summation changed to an integral so that equation [1.46] is rewritten as

$$M_L = \frac{K^2 \hbar}{2mN} \frac{1}{8\pi^3} \iiint_V \frac{(\bar{n}_q + \frac{1}{2})}{\omega_q} d^3q \quad . \quad [1.48]$$

Changing to spherical coordinates which are more appropriate to the Debye model, we obtain

$$M_L = \frac{K^2 \hbar}{2mN} \frac{1}{8\pi^3} \int_0^{q_M} \frac{(\bar{n}_q + \frac{1}{2})}{\omega_q} 4\pi q^2 dq \quad . \quad [1.49]$$

Using equations [1.41] and [1.43], the variable of integration can be changed to ω :

$$M_L = \frac{K^2 \hbar}{2mN} \frac{1}{8\pi^3} \int_0^{\omega_M} \frac{(\bar{n}_q + \frac{1}{2})}{\omega_q} \frac{4}{3}\pi q_M^3 D(\omega) d\omega \quad . \quad [1.50]$$

The volume of the Debye sphere ($\frac{4}{3}\pi q_M^3$) is equal to the number of states in it (N) divided by the density of states ($\frac{1}{8\pi^3}$):

$$\frac{4}{3}\pi q_M^3 = N 8\pi^3 \quad . \quad [1.51]$$

Incorporating the Debye spectrum from equation [1.43] M_L

can now be written as

$$M_L = \frac{K^2 \hbar}{2m} \int_0^{\omega_M} \left(\frac{1}{e^{\hbar\omega/kT} - 1} + \frac{1}{2} \right) \frac{3\omega}{\omega_M^3} d\omega \quad [1.52]$$

Changing variables to $z = \hbar\omega/kT$ results in

$$M_L = \frac{3\hbar^2 K^2 T^2}{2m k \theta_M^3} \int_0^{\frac{\theta_M}{T}} \left(\frac{1}{e^z - 1} + \frac{1}{2} \right) z dz \quad , \quad [1.53]$$

where we have utilized the relation

$$\hbar\omega_M = k\theta_M \quad , \quad [1.54]$$

which relates the Debye temperature θ_M and the Debye frequency ω_M . M_L can be written now as

$$M_L = \frac{3K^2 \hbar^2 T}{2mk\theta_M^2} \left(\phi\left(\frac{\theta_M}{T}\right) + \frac{\theta_M}{4T} \right) \quad , \quad [1.55]$$

where

$$\phi\left(\frac{\theta_M}{T}\right) = \frac{T}{\theta_M} \int_0^{\frac{\theta_M}{T}} \frac{z dz}{e^z - 1} \quad . \quad [1.56]$$

Finally by using equation [1.39] to substitute for K we obtain

$$M_L = \frac{24\pi^2 \hbar^2 T}{mk \theta_M^2} \left(\phi\left(\frac{\theta_M}{T}\right) + \frac{\theta_M}{4T} \right) \frac{\sin^2 \theta}{\lambda^2} \quad [1.57]$$

or

$$M_L = \frac{6 \hbar^2 T}{mk \theta_M^2} \left(\phi\left(\frac{\theta_M}{T}\right) + \frac{\theta_M}{4T} \right) \frac{\sin^2 \theta}{\lambda^2} \quad . \quad [1.58]$$

To summarize the results of the calculation of a scattering matrix, the structure factor can be reduced to a sum over the lattice sites L of an exponential dependent only upon the rest position of the atom times another exponential

that accounts for the thermal vibration of the atom at site L :

$$SF = \sum_L e^{-ik \cdot L} e^{-M_L} . \quad [1.59]$$

Thus the scattering matrix can be written as

$$M_{\vec{k} \leftarrow \vec{k}} = \sum_L e^{-ik \cdot L} f_L(K) e^{-M_L} . \quad [1.60]$$

The final result of this analysis is that for an ideally imperfect crystal the intensity of Bragg diffraction (I) is given by

$$I \propto |M_{\vec{k} \leftarrow \vec{k}}|^2 . \quad [1.61]$$

The above discussion assumed that the lattice is composed of only one type of atom. The crystals studied in this work were composed of two atoms. Therefore, the electron density is not necessarily periodic and atoms can be permanently displaced from their regular site. As a result, each term in the lattice sum of equation [1.19] must be considered a function of the lattice site L . Each site L has a characteristic atomic scattering factor f_L and its own characteristic vibration amplitude U_L . The atomic scattering factor for each site in an alloy, of course, cannot be calculated exactly. Instead the approximation is made that the atom in the alloy scatters like a free atom with the same valence. Thus, the integral in equation [1.20] is replaced by an integral where $\rho_a(r)$ is for a free atom and the integration is carried out over the volume of the free atom. Thus, the scattering factor is assumed

dependent only upon which type of atom is located at the site L . U_L is dependent not only upon the type of atom at site L , but also upon the environment around the L th atom. Because of the size differences between atoms, U_L can have a static displacement from its lattice point in addition to its dynamic displacement.

Huang (1947) originally treated the effect of the static displacements on the diffracted intensity. It was assumed that each site in the crystal lattice is occupied by a spherically symmetric distortion center dependent upon the atom occupying the site. The lattice is also assumed to react as though it was an isotropic medium. With these assumptions the effect of distortion can be reduced to a term of the form

$$1 - 2M_{St} \approx \exp -2M_{St} , \quad [1.62]$$

where M_{St} is a term analogous to the thermal displacement Debye-Waller factor. Sparks and Borie (1966) have extended this analysis to displacements that are not parallel to the interatomic vector. Thus, the Debye-Waller factor M for alloys contains both a contribution from dynamic and static displacements. The effect of both types of displacement on the Bragg intensities is to decrease the magnitude of the diffracted intensity, but to leave the width of the peak unaffected. $M_{\vec{k}}, \vec{k}$ can be written as the sum in equation [1.60], but the probability $P_x(L)$ of the L th site being filled by a x atom must be included:

$$M_{\vec{k}} = \sum_L P_A(L) e^{-i\vec{k} \cdot \vec{L}} f_A(\vec{k}) \exp(-M_A) + P_B(L) e^{-i\vec{k} \cdot \vec{L}} f_B(\vec{k}) \exp(-M_B) , \quad [1.63]$$

where each type atom is assumed to have a characteristic temperature factor. In equation [1.63] the assumption is made that the environment around each type of atom is the same.

For Bragg diffraction from disordered homogeneous solid solutions Guinier (1963) points out that the diffraction pattern is identical to that of a crystal having the same lattice with identical average atoms. The scattering factor for the average atom (f_{av}) times the exponential of the average Debye-Waller factor M_{av} is given by:

$$f_{av} \exp(-M_{av}) = P_A f_A \exp(-M_A) + P_B f_B \exp(-M_B) . \quad [1.64]$$

The nonperiodicity does produce a diffuse scattering which is dependent upon the lattice distribution. The study of the diffuse scatter to obtain the atomic distribution is covered in the books by Guinier (1963) and Warren (1969).

In some solid solutions at certain compositions it is possible for the atoms to form a regular periodic sequence. Because of the new period new diffraction lines occur called superlattice lines. The scattering matrix of these lines is also given by equation [1.60]. In ordered

diatomic lattices there is an optic mode of vibration in addition to the acoustic mode. As is discussed in section 3.2, this leads to anisotropic lattice vibrations in certain cases. This, of course, makes the substitution of a Debye spectrum for the real spectrum seem questionable. The approximation is made that each atom can have a characteristic Debye temperature and that temperature can be dependent upon the direction in the lattice. The individual Debye temperatures or thermal displacements can be separated as is discussed in Chapter II.

1.3 Thermal displacements in disordered Cu-Au alloys

Passaglia and Love (1955) have determined the electrical resistivity Debye temperature (θ_R) for polycrystalline disordered Cu-Au alloy wires at 75°K. This data, along with that of other authors to be discussed later, is presented in Table 1.1. As discussed by Blackman (1951) the electrical resistivity Debye temperature results from only the longitudinal modes of vibration, where as the X-ray Debye temperature (θ_M) results from both the longitudinal and transverse modes. Thus, one cannot expect the θ_R and θ_M values to be exactly the same. Recognizing this difference the data of Passaglia can still be used to provide information on the thermal displacements in Cu-Au solid solutions. The values of θ_R have been converted into mean

TABLE 1.1

DEBYE TEMPERATURES AND THERMAL DISPLACEMENTS
FOR DISORDERED Cu-Au ALLOYS AT 298°K

COMPOSITION	θ_D °K	$\langle U_s^2 \rangle^{1/2}$ Å	AUTHOR
Cu	326.	.0814	Passaglia (1955)
.75Cu-.25Au	244.	.0874	↓
.625Cu-.375Au	226.	.0870	
.5Cu-.5Au	212.	.0866	
.375Cu-.625Au	202.	.0855	
.25Cu-.75Au	186.	.0879	
Au	175.	.0851	
Cu	311.	.0852	Webb (1962)
Cu	325.	.0817	↓
.92Cu-.08Au	284.	.0861	
.85Cu-.15Au	270.	.0853	
.75Cu-.25Au	254.	.0841	
.75Cu-.25Au	271.	.0754	Owen (1967)

square thermal displacements (\overline{U}_s^2) at 298°K with the Debye theory from James (1948)

$$\overline{U}_s^2 = \frac{3\hbar}{mk\theta^2} T \left\{ \phi(x) + \frac{x}{4} \right\}, \quad [1.65]$$

where m is taken to be an arithmetic average of the constituent masses, $x = \theta/T$ and $\{\phi(x) + x/4\}$ is a function defined in equation [1.56].

Owen and Evans (1967) determined that a sintered powder of disordered Cu_3Au had a X-ray Debye temperature (θ_M) of 271°K. They measured the integrated intensity from a Bragg diffraction peak at room temperature and at an elevated temperature. The Debye temperature was corrected for variation with temperature on the basis of the Grüneisen relation. The data was taken with a Co filtered Ni continuous spectrum with film recording techniques. This is a very difficult experiment to perform. Several reasons for this are that for a powder the diffracted intensity is low in comparison with the diffracted and scattered continuous background. This makes it difficult to evaluate the background under the peak. When using film techniques it is difficult to obtain better than 5 percent reproducibility from intensity measurements, as shown by Dozier *et.al.* (1967). Furthermore, it is difficult to eliminate the $\lambda/2$ component of the continuum which is a second order diffraction to the same spot of the film as the first order λ .

Webb (1962) determined the X-ray Debye temperatures for Cu-Au alloy powders of composition ranging from Cu to

Cu_3Au . Webb plotted the log of an adjusted intensity for many reflections against $(\sin\theta/\lambda)^2$. The resulting slope gives the Debye-Waller factor from which the thermal displacements and Debye temperature can be determined. By doing this at room temperature and at liquid nitrogen temperature, the static displacements are eliminated. It was assumed unjustifiably in the analysis of the data that the Debye temperature is independent of temperature. The thermal diffuse scatter was evaluated by the technique of Chipman and Paskin (1959 A&B). The measurement on the powders was made with polychromatic Mo radiation. Electronic methods with pulse height analysis were used to record the data. This eliminates the $\lambda/2$ contribution, but again the accuracy is limited by the difficulty of obtaining a strong signal from the powder above the scattered and diffracted continuum.

It would be desirable to have this existing data fit together to present a unified picture of the effects of alloying on the thermal displacements of disordered Cu-Au alloys. However, the only composition which is in common to all of the above work is the nonequilibrium quenched Cu_3Au . The Debye temperatures for this alloy measured by Passaglia, Owen and Webb are 244°K , 271°K , and 254°K respectively. Also, Webb only studied compositions from Cu to Cu_3Au , and Passaglia had no measurements between these limits. For the Debye temperature of pure Cu Passaglia obtained 326°K and Webb obtained values from 311°K to 325°K which is good agreement.

In an attempt to correlate the existing data it was decided to study the following samples:

- (a) Pure Cu: to tie this work to other work done on Cu such as that of Flinn *et.al.* (1961), Webb and Passaglia;
- (b) .90 Cu-.10Au: to compare with Webb's work;
- (c) 75Cu-.25Au: to compare with all of the above authors and
- (d) 2Cu-.8Au: to compare with Passaglia's data.

It was hoped that the study of these alloys would permit bringing these divergent sets of data into accord to determine the effect of alloying on the thermal displacements in solid solutions.

1.4 Thermal displacements in ordered Cu₃Au alloys

Several measurements of the thermal displacements of individual copper and gold atoms have been made as shown in Table 1.2, the most recent and seemingly the most reliable being those of Gehlen and Cohen (1969). These measurements were made on crystals with a long range order parameter (S) of [1.0], using the technique described in section 2.9 with crystal monochromated Mo K_{α} radiation. The intensities were corrected for thermal diffuse scatter as described by Schwartz and Cohen (1965). The reason for the disagreement between Flinn's (1960) data and that of Gehlen and Cohen is not obvious. One difference is that

TABLE 1.2
ROOM TEMPERATURE THERMAL DISPLACEMENTS
IN Cu_3Au CRYSTALS

S	$\left\langle \overline{U_s^2} \right\rangle_{\text{Cu}}^{1/2}$	$\left\langle \overline{U_s^2} \right\rangle_{\text{Au}}^{1/2}$	Author
.80	.093 Å	.069 Å	Chipman (1956)
.94	.088	.068	Flinn (1960)
1.00	.095	.082	Schwartz (1965)
1.00	.099	.084	Gehlen (1969)

Flinn investigated a $S = 0.94$ crystal, and the dependence of the thermal displacements on the degree of order is not clearly understood. Also in partially ordered crystals, the technique used by Flinn results in the static displacements contributing to the Debye-Waller factor as is discussed in section 2.5. Chipman (1956) also studied a partially ordered Cu_3Au crystal ($S=0.8$) by this same technique and no correction was made for static displacements. Chipman did not crystal monochromate the Mo K_α radiation, and he did not make any thermal diffuse scattering correction. For these reasons Chipman's data is questionable.

No study has been made of the effects of the degree of order on the thermal displacements. The evaluation of the vibrational entropy changes with ordering is an important part of the present study. Also, the thermal displacements will provide data on the changes in the interatomic force constants during ordering. The directional dependence of the thermal displacements was also investigated as a function of the degree of order. In the past it has been assumed that the thermal displacements of all cubic crystals were isotropic. This has been demonstrated for primitive monatomic cubic lattices as is discussed in Maradudin *et.al.* (1963). This assumption cannot be extended to ordered Cu_3Au lattice; although, this is not generally recognized.

CHAPTER II

EXPERIMENTS

2.1 Introduction

As stated earlier the central objective of these experiments was to determine the value of the thermal displacements in single crystals of Cu-Au alloys. The single crystals were characterized by determination of the lattice parameter, the homogeneity, and for ordered crystals the degree of long range order S .

2.2 Specimen preparation and analysis

The Cu, and the Cu₃Au ($S = 1.0$) crystals were purchased from Monocrystals, Incorporated of Cleveland, Ohio. The other alloy crystals were grown in a Materials Research Corporation Model Z-83 Zone Melting apparatus, equipped with a Marshall 4030 Control Console, a Marshall High Temperature Furnace (1200°C), a Cenco Supervac OD-25 diffusion pump, a Cenco Hyvac 2 forepump, a Cenco thermocouple vacuum gauge and a Cenco ionization gauge. The apparatus was used both for the growth of the crystals and subsequent homogenization.

The starting materials were 99.999 Au and 99.999 Cu purchased from A.D. McKay and Sigmund Cohn. Randomly oriented crystals approximately 1 inch in length and 1/2 inch diameter were grown by normal freezing of the molten ingot in a graphite crucible. The vacuum was 1×10^{-5}

microns and the furnace travel was approximately 1/2 inch per hour. An etch was used to check the monocrystallinity of the prepared crystals. An aqua regia etch was used for the 80 at.% Au- 20 at.% Cu crystal and a solution of 50ml. distilled water, 50 ml. HNO_3 and 0.5gm AgNO_3 was used for the other alloys. The crystal was then mounted on a brass rod with Duco cement, and oriented on a Norelco X-ray unit by the Laue back reflection method. A Metals Research Servomet spark cutter with a continuously fed copper wire was used to cut the crystals into rectangular specimens with sides (110), (110), and (001) to within 1° of the [110]. For the annealing treatment the crystals were then placed in a closed graphite mold or packed in graphite chips, placed in a Vycor tube and evacuated to 1×10^{-7} microns before sealing off. The annealing schedule is shown in Table 2.1.

2.3 Equipment

A General Electric XRD-6 X-ray diffractometer was the basic instrument used in these experiments. A schematic of the experiment setup is shown in Figure 2.1. The beam from the X-ray tube was monochromated with a doubly bent LiF crystal which was set to diffract the $K_{\alpha_1} - K_{\alpha_2}$ doublet. The specimen holder was mounted on a special Ω motion attachment (model #A7018AG from Electronics & Alloys, Inc.) which allowed setting Ω to about 0.002° .

The X-ray detection system was selected for low noise and high stability. The detector for Cu K_α radiation was

TABLE 2.1
ANNEALING SCHEDULE OF THE Cu-Au ALLOYS
COMPOSITION IN ATOMIC PERCENT

SAMPLE	HEAT TREATMENT		ENCAPSULATION
91Cu-09Au(a)	700°C 400°C furnace cooled	74 hrs. 52 hrs.	closed graphite mold, evacuated Vycor tube
Cu ₃ Au(S = 0.0)	678°C 410°C quenched in water	64 hrs. 48 hrs.	graphite chips, evacuated Vycor tube
Cu ₃ Au(S = 0.53)	550°C 288°C quenched in water	3 hrs. 4 hrs.	evacuated Vycor tube
Cu ₃ Au(S = 0.80)	678°C 415°C 357°C quenched in water	48 hrs. 96 hrs. 1 1/2 hrs.	graphite chips, evacuated Vycor tube
Cu ₃ Au(S = .98)	684°C 370°C 300°C 245°C 173°C furnace cooled	48 hrs. 99 hrs. 63 hrs. 74 hrs. 112 hrs.	evacuated Vycor tube
80Au-20Cu	630°C furnace cooled	88 hrs.	graphite crucible under vacuum
91Cu-09Au(b)	750°C 600°C 450°C 300°C 120°C Furnace cooled	216 hrs. 168 hrs. 168 hrs. 144 hrs. 100 hrs.	Vycor tube graphite crucible under vacuum

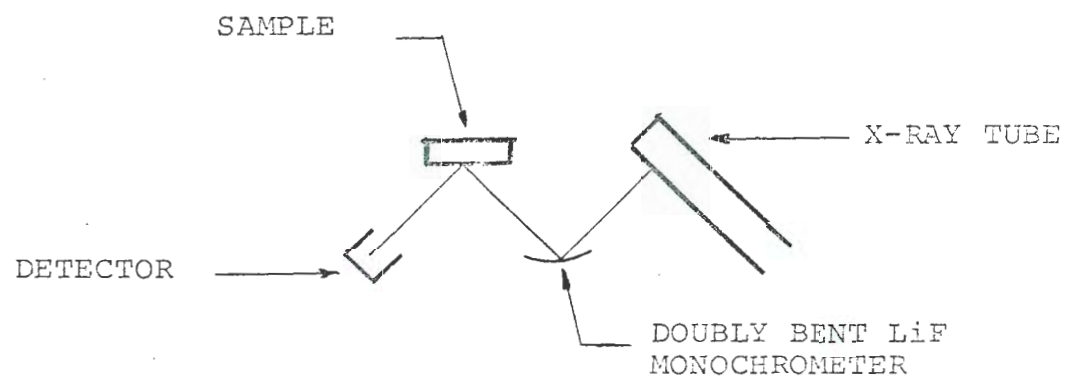


FIGURE 2.1 SCHEMATIC OF X-RAY
DIFFRACTION EXPERIMENT

a Xenon filled sealed proportional counter (G.E. SPG-8), and for Ag K_{α} radiation a Harshaw Scintillator was used. The detector bias potential was provided by a Baird Atomic Super Stable high voltage power supply model 312A. This provides a constant potential to within $\pm 0.02\%$. The Xenon detector preamplifier (ORTEC 109PC) utilized a field effect transistor for low noise amplification of the detector signal. The amplifier (ORTEC 485) was set so that the peak of the pulse distribution was at 5 volts on the 0 to 10 volt scale of the single channel analyzer (ORTEC 406A). The lower limit of the discriminator was set at 2.5 volts and the upper limit was set at 7.5 volts. The 2.5 volt level of the discriminator eliminated low energy noise and the 7.5 volt setting of the upper level discriminator eliminated the $\lambda/2$ component of the diffracted continuum which would peak at 10 volts. The signal was then sent to a digital ratemeter (ORTEC 434) which can be used either as a ratemeter, scaler, or timer. The output from the digital ratemeter was then sent through a print out control (ORTEC 432) to a teletype print out.

2.4 Determination of lattice parameter, composition and homogeneity

The samples had to be characterized as to composition, homogeneity, and degree of order before measurements of thermal displacements were made. Copper K_{α} radiation was used for this work unless noted otherwise. The composition was determined by measuring the lattice parameter and

comparing it to published data of composition versus lattice parameter for the Cu-Au. The homogeneity was determined by measuring the lattice parameter at several locations along the crystal face.

The procedure for measuring the lattice parameter was similar to that discussed by Schwartz *et.al.* (1964). The crystal was mounted on a goniometer (Electronics and Alloys, Inc. Model #63-12-CM). The goniometer allowed X, Y and Z translation and χ rotation. These motions are shown in Figure 2.2. χ is rotation about the Y axis. Ω rotation about the Z axis was provided by a special goniometer (Electronics and Alloys, Inc. Model #A7018AG) which permitted setting Ω to about 0.002° .

To obtain accurate lattice parameters proper alignment of the diffractometer is necessary. The following technique assured the the X-ray beam, the sample face, the axis of rotation of the goniometer, and the slits were all collinear when θ was set at 0° . The axis of rotation of the goniometer was considered as fixed, and the X-ray tube and detector slits were aligned collinear to the goniometer axis. This was made possible by hand operated screws on the X-ray tube housing that provided X and Y motion for the X-ray tube. The steps in the alignment are as follows:

- A. Make the X-ray beam pass over the axis of rotation of the goniometer. The steps necessary to achieve this are:

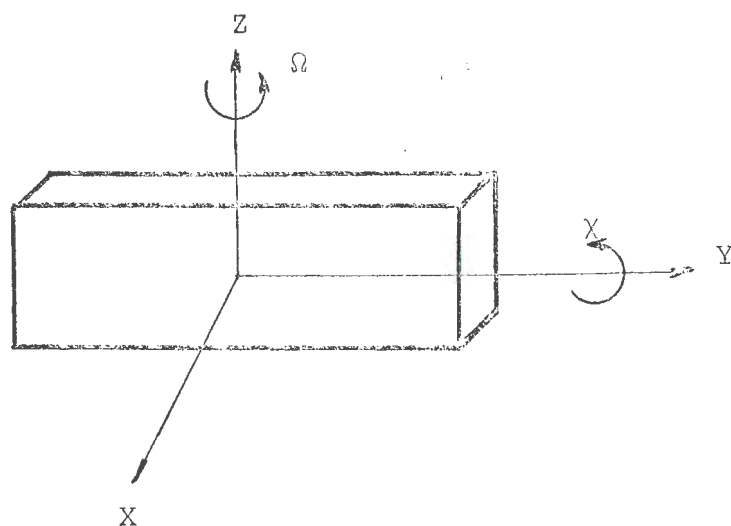


FIGURE 2.2 DEGREES OF FREEDOM FOR THE SAMPLE

1. Move the crystal along the Y axis to the center of the X-ray beam. This is checked by noting when the zero beam intensity is decreased by 50 percent. Slits were not used in this step, and an attenuator is required to reduce the intensity.
2. Check that the crystal is parallel to the X-ray beam by rotating the crystal back and forth with the Ω rotation. When the crystal is parallel to the X-ray beam the recorded intensity will decrease with rotation in either direction. The setting at which the crystal is parallel to the X-ray beam is determined by first roughly determining the position. Then the crystal is rotated in both a plus and minus direction until about $3/4$ of the maximum intensity is obtained, and the angles noted. It is important that the intensities on either side of the center position be the same to within about 1 percent. The desired setting was then midway between the two settings at $3/4$ of the center position intensity.
3. Check that the X-ray beam goes through the axis of rotation of the goniometer. This is done by rotating the crystal exactly 180° with the Ω motion. If the intensity is the same after 180° rotation as before (50 percent of full zero beam) then the goniometer axis lies in the crystal face.

If this is not the case, then the X-ray beam must be moved in the direction of the axis of the goniometer with the X and Y motion provided by hand screws on the X-ray tube housing. The amount and direction of movement can be estimated from the intensity i.e., move the tube to change the intensity by 50 percent of the difference between what the intensity reading was and what it should have been. Then repeat steps 1, 2, and 3 above until the intensity does not change after 180° rotation of the crystal. When this condition is satisfied the X-ray beam is passing over the center of the axis of rotation of the goniometer.

- B. Make the aperture used for the lattice parameter measurement symmetric about the zero angle beam. At this point of the alignment procedure apertures were placed on the detector. The goniometer was set at plus and minus 0.2° from zero degrees. The aperture is centered on the zero beam when equal intensities are obtained on either side of zero degrees. If further adjustment is required several techniques may be used. Usually there was enough tolerance in the holes of the aperture plates that they could be adjusted and reset with thickness gauges. At times it was necessary to put shims behind the aperture holder. It is important to note that the particular aperture to be used for lattice parameter measurements must be used in the alignment, for each aperture is set slightly different.

To determine accurate lattice parameters, the crystal must be properly aligned in the diffractometer. First the crystal is put at the center of the X-ray beam and aligned parallel to the zero angle X-ray beam as described in A.1 and A.2 above. The goniometer is then put to the expected Bragg diffraction angle. Because the crystal planes are generally not exactly parallel to the crystal face, it is necessary to change χ and Ω to obtain the approximate peak maximum. A specific procedure was then used to precisely align χ and Ω to the proper values. First χ was set by noting the angles at which the intensity was $3/4$ of the maximum intensity on either side of the peak. An integration time on the scalar of ten seconds was used to accurately determine the equal intensity positions on either side of the peak. The proper angle is the mean of the angles at the two equal intensity positions. The proper 2θ position is found by a similar technique, but Ω has to be adjusted to a peak value in the process for each equal intensity position on the 2θ scale. If a particular value of Ω is set, 2θ could be peaked, but unless 2θ is at exactly the correct value, a false peak would be obtained. But if 2θ is peaked for each Ω position then the true maximum results. Once the true 2θ maximum is found, then Ω can be set in the same way as χ .

A θ - 2θ scan was used to obtain the lattice parameter. The digital rate meter was used in the one second

integration mode, the goniometer was operated with the slowest possible speed $0.2^{\circ}/\text{min.}$, and the strip chart recorder was operated at its fastest speed 60 in./hr. To obtain precision lattice parameters, it was necessary to eliminate any play from the goniometer and strip chart recorder. If either is set at the position desired, and the goniometer then turned on, it takes several seconds before the play in the mechanical system is taken up and the precise coordination between the goniometer and strip chart recorder is lost. To eliminate this, the setting on the goniometer was first moved back several hundredths of a degree from the desired starting position. Then the goniometer motor was turned on so that all of the gears were engaged, and then it was stopped at the desired starting angle. The same procedure was then used to set the starting position of the strip chart recorder.

The lattice parameter (a) was obtained as follows. The diffraction scans from a crystal face were recorded for as many reflections as possible. The 2θ value for any particular peak was determined by extrapolating the mean value of 2θ to the peak maximum. The interplanar spacing d_{hkl} for the hkl set of planes could be determined with Bragg's law:

$$\lambda = 2 d_{hkl} \sin \theta \quad .$$

A value for the lattice parameter can be determined from each reflection, but as is discussed in Cullity (1956)

the errors in the measurement are minimized as the Bragg angle (θ) approaches 90° . Thus, if the lattice parameter measured from each reflection (hkl) is plotted against some function of the Bragg angle (θ); then at $\theta=90^\circ$ the measurement will correspond to a minimum of experimental error. The lattice parameters in this work were established from an extrapolation to $\cos^2\theta=0$. The diffractometer alignment was tested through a determination of the well established lattice parameter of LiF ($a=4.0267$) as given in the General Electric tables (1959). The results of this measurement and the lattice parameters for the Cu-Au alloy crystals are shown in Table 2.2.

The lattice parameter (a) was used to determine the crystal composition by comparison with previous measurements of composition versus lattice parameter as is shown in Figure 2.3. The homogeneity was determined by measuring the Bragg angle (θ) at a minimum of three locations along the crystal face. The variation in the diffraction angle $\Delta\theta$ results in the change in interplanar spacing Δd_{hkl} by differentiating Bragg's law to obtain:

$$\Delta d_{hkl} = d_{hkl} \cot \theta \Delta\theta$$

The percent change in composition across the crystal was obtained by determining Δd_{hkl} and determining the change in composition associated with Δd_{hkl} from Figure 2.3.

TABLE 2.2

X-RAY ANALYSIS OF Cu-Au ALLOYS

Composition in atomic percent, lattice parameter in Angstroms, and density in grams per centimeter cubed. Uncertainties in the density are due to assuming a one percent accuracy in the atomic compositions.

SAMPLE	COMPOSITION FLUCTUATIONS IN PERCENT	LATTICE PARAMETER	DENSITY
91Cu-09Au (b) ¹	.180	3.6585	10.00 ± .01
Cu ₃ Au (S = 0.0)	.140	3.7488	12.13 ± .17
Cu ₃ Au (S = 0.53)	.130	3.7457	12.17 ± .17
Cu ₃ Au (S = 0.80)	.077	3.7505	12.20 ± .17
Cu ₃ Au (S = .98)	.100	3.7426	12.26 ± .17
80Au-20Cu	.300	3.9987	17.70 ± .14
LiF	--	4.0270	--

1. After heat treatment (a) the lattice parameter of this crystal was 3.6623Å (see Table 2.1)

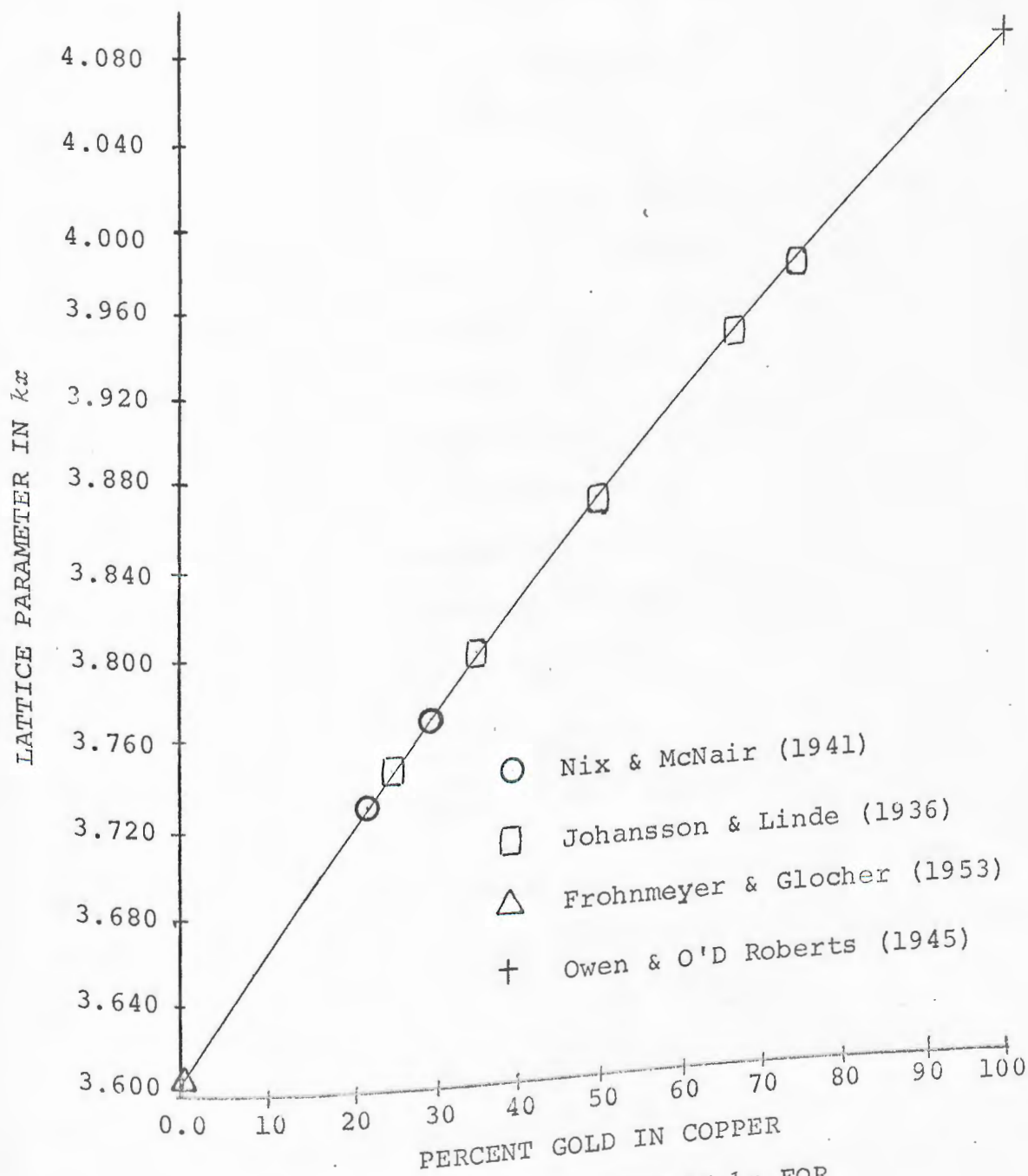


FIGURE 2.3 LATTICE PARAMETER IN kx FOR
Cu-Au ALLOYS

2.5 Determination of long range order parameter in Cu_3Au alloys

For the .75Cu-.25Au alloys the long range order parameter S was determined. A value of S was obtained by measuring the integrated intensity of a fundamental and a superlattice reflection. From Warren (1969):

$$S^2 = \frac{I_s F_f^2 L_p(f) \exp(-2M_f)}{I_f F_s^2 L_p(s) \exp(-2M_s)} \quad [2.1]$$

where I_s/I_f is the ratio of the integrated intensities of the superlattice and fundamental reflections corrected for thermal diffuse scattering and constant background by the technique of Skelton and Katz (1969). F , the scattering factor, is discussed in section 2.9. The Thomas-Fermi scattering factors from the International Crystallographic Tables (1955) were corrected for anomalous dispersion with the data of Dauben and Tempelton (1955). The Lorentz-Polarization factor (L_p) is given by

$$L_p = \frac{1 + (\cos^2 2\theta_{\text{LiF}} \cos^2 2\theta_{\text{Cu}_3\text{Au}})}{(1 + \cos^2 2\theta_{\text{LiF}}) (2 \sin^2 \theta_{\text{LiF}} \sin^2 \theta_{\text{Cu}_3\text{Au}})} \quad , \quad [2.2]$$

where $2\theta_{\text{LiF}}$ is the diffraction angle for CuK_α from the LiF monochromator and $2\theta_{\text{Cu}_3\text{Au}}$ is the diffraction angle from the Cu_3Au sample.

The values of M_s , M_f , I_s and I_f were determined experimentally. The details of determining these values are covered in section 2.7, but briefly the experiment was as

TABLE 2.3
EXPERIMENTAL VALUES FOR THE DETERMINATION OF S

RESULTANT S	M_{300}	M_{400}	I_{300}	I_{400}
.98	.118	.177	14839	75249
.80	.078	.158	13051	92638
.53	.072	.142	8571	137922

follows. The sample was clamped in a cryostat and then the diffractometer was aligned the same as for lattice parameter measurements. I_s and I_f , the total integrated intensities, were recorded at both room temperature and liquid nitrogen temperature. The intensities were then corrected for constant background and for thermal diffuse scattering with the technique of Skelton and Katz (1969). Table 2.3 shows the resultant intensities, M values, and S .

2.6 Introduction to measurement of thermal displacements in Cu-Au alloys

The main objective of the experimental part of this study was to determine the mean square thermal displacements in Cu-Au disordered alloys. The relationship of the thermal displacements to the intensity of X-rays diffracted from a crystal is presented in James (1948). The ratio of the intensity I_0 measured with the atoms at rest to the intensity I_1 measured at some temperature T_1 is given by

$$I_1/I_0 = \exp -2M \quad , \quad [2.3]$$

where $2M$ is the Debye-Waller factor. M can be expressed in terms of the mean square thermal displacements $\overline{U_s^2}$ in the \overline{s} direction by

$$M = 8\pi^2 \overline{U_s^2} \left(\frac{\sin\theta}{\lambda} \right)^2 \quad . \quad [2.4]$$

It is impossible to measure I_0 directly because the atoms cannot be completely immobilized, but I_0 can be eliminated by taking the log of the ratio of the intensity measurements at two temperatures:

$$\ln \frac{I_{T_1}}{I_{T_2}} = -2 (M_{T_1} - M_{T_2}) . \quad [2.5]$$

There is still one equation and two unknowns $\overline{U}_s^2(T_1)$ and $\overline{U}_s^2(T_2)$. To circumvent this problem the thermal displacements are expressed in terms of the Debye temperature as was developed in section 1.2

$$\overline{U}_s^2 = \frac{3h^2 T}{4\pi^2 m k \theta_M^2} \left[\phi(X) + \frac{X}{4} \right] , \quad [2.6]$$

where θ_M is the X-ray Debye temperature, $\phi(X) + X/4$ is a temperature factor defined in equation [1.56], X is θ_M/T , and $\phi(X)$ can be approximated by

$$\phi(X) = 1 - \frac{X}{4} + \frac{X^2}{36} - \frac{X^3}{3600} + \dots . \quad [2.7]$$

θ_M is in general a function of temperature; therefore, there are still two variables. The number of variables can be reduced to one by expressing the Debye temperature as a function of temperature.

The change in the Debye temperature with temperature can be expressed in terms of the Grüneisen constant. The basic definition of the Grüneisen constant (γ), as discussed by Ziman (1964), is that γ relates the change in frequency $d\nu$ for every mode to the change in volume dV through the relationship

$$\frac{d\nu}{\nu} = \gamma \frac{dV}{V} . \quad [2.8]$$

If we assume that the Debye model is valid we can write

$$\frac{d\nu_M}{\nu_M} = \gamma \frac{dV}{V} \quad . \quad [2.9]$$

From the relationship

$$h\nu_M = k\theta_M \quad , \quad [2.10]$$

equation [2.9] can be rewritten as

$$\frac{d\theta_M}{\theta_M} = \gamma \frac{dV}{V} \quad . \quad [2.11]$$

The coefficient of linear expansion is written as

$$\alpha = \frac{1}{3} \frac{1}{V} \frac{dV}{dT} \quad . \quad [2.12]$$

Therefore, equation [2.11] can be rewritten as,

$$\frac{d\theta_M}{\theta_M} = 3\alpha\gamma dT \quad . \quad [2.13]$$

If the temperature is changed from T_1 to T_2 , upon integration the result is

$$\ln \frac{\theta_M(T_2)}{\theta_M(T_1)} = 1 - \frac{\theta_M(T_2)}{\theta_M(T_1)} = 3\alpha\gamma(T_2 - T_1) \quad , \quad [2.14]$$

or

$$\theta_M(T_2) = \theta_M(T_1) [1 - 3\alpha\gamma(T_2 - T_1)] \quad . \quad [2.15]$$

This is the same result obtained by Owen and Williams (1947).

This reduces the number of variables to one, i.e. the Debye temperature at room temperature.

Substituting equations [2.15], [2.6] and [2.7] into equation [2.5], $\theta_M(T_1)$ can be solved for:

$$\theta_M(T_1) = \left[B_{T_1} \phi(X)_{T_1} - \frac{B_{T_2} \phi(X)_{T_2}}{[1+3\alpha\gamma(T_1-T_2)]} \right] / \left[\frac{M_{T_2} - M_{T_1}}{A} - \Delta \right], \quad [2.16]$$

where

$$B_T = \frac{T}{4d_{hkl}^2(T)}, \quad A = \frac{6h^2}{mk}, \quad \text{and } \Delta = \frac{1}{16} \left(\frac{\theta_M(T_1)^{-1}}{d_{hkl}(T_1)} - \frac{\theta_M(T_2)^{-1}}{d_{hkl}(T_2)} \right).$$

$\phi(X)$ is a function of $\theta_M(T_1)$, thus it is necessary to solve for $\theta_M(T_1)$ by an iterative process. The iterative process was continued until successive calculations of $\theta_M(T_1)$ differed by less than 0.1 degree. The values of α and γ were taken from Kittel (1967). For alloys a molar average was used for the values of α , γ and m . The α and γ are terms used in the small temperature dependence correction for θ_M , thus the error in an assumption of a molar average of α and γ has little effect on the value of θ_M . This is not the case with m which is inversely related to θ_M . In most cases a molar average is used for m , but it has also been suggested by Krivoglaz (1969) that the inverse mass can be averaged. For this reason \bar{U}_s^2 was chosen as the more fundamental parameter, θ_M is only used to calculate \bar{U}_s^2 through equation [2.6]. A study of equation [2.6] and [2.16] shows that the value chosen for m essentially cancels out of the equations for \bar{U}_s^2 .

The Debye-Waller factor (M) has both thermal (M_{Th}) and static (M_{St}) components. After Huang (1947) M can be written as

$$M = M_{Th} + M_{St} \quad . \quad [2.17]$$

Taking the log of the intensity ratio at two temperatures as in equation [2.5] results in

$$\ln \frac{I_{T_1}}{I_{T_2}} = -2 \left(M_{Th}(T_1) - M_{Th}(T_2) \right) - 2 \left(M_{St}(T_1) - M_{St}(T_2) \right). [2.18]$$

M can be expressed in terms of a static displacement analogous to the thermal displacements in equation [2.6]. The static displacements can be assumed to be nearly independent of temperature, thus the second term on the right-hand side of equation [2.18] is very small in comparison to the first term and can be disregarded. Thus, the measurement of intensities at two temperatures eliminates the static displacements. M will be used as the Debye-Waller factor for thermal displacements in the remainder of the text.

2.7 Experimental techniques for the measurement of thermal displacements by the two temperature method

The intensities were measured on the XRD-6 diffractometer described in section 2.3. The addition of a cryostat which mounted directly on the special ω motion goniometer allowed measurement of the intensity at various temperatures. Figure 2.4 shows a schematic of the model CT-36 cryostat manufactured by Cryogenic Associates. The rectangular samples were clamped in a split copper block, this

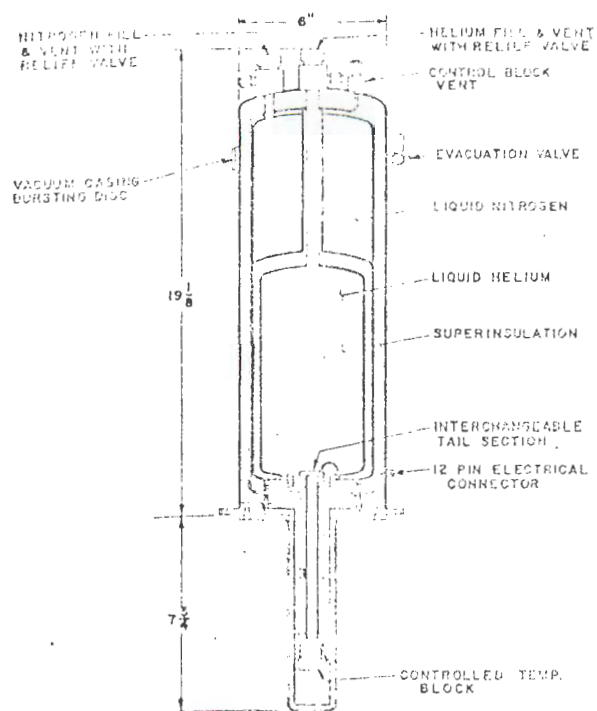
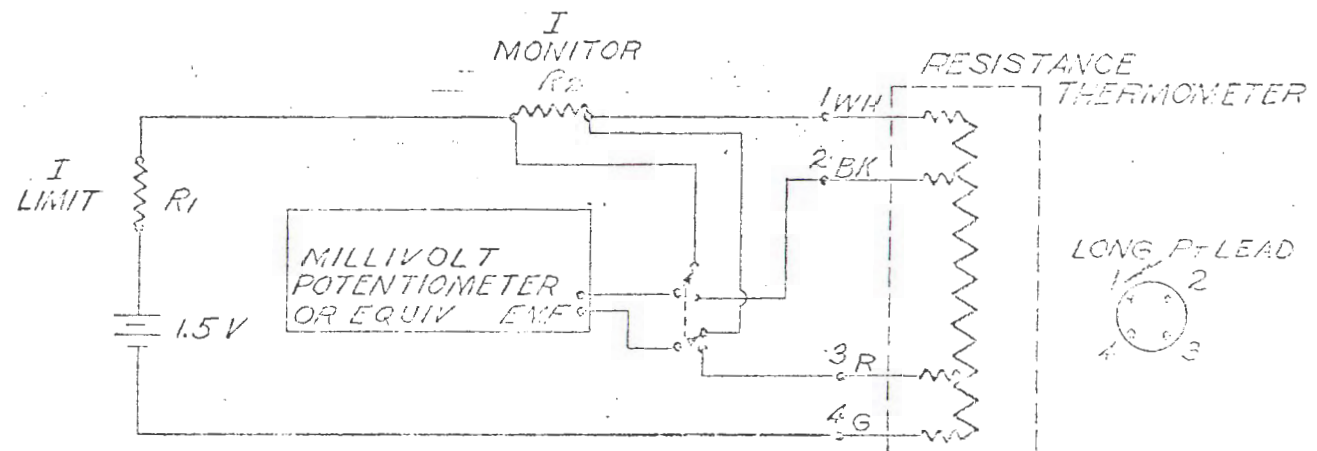


FIGURE 2.4 SCHEMATIC OF CRYOSTAT

assured intimate thermal contact with the upper block which was in contact with the coolant. The cylindrical Cu crystal was clamped by a set screw for intimate thermal contact in a hole machined to a slip fit in a copper block. The liquid nitrogen coolant was forced by the pressure of its own gas through a small vent tube. The tube passed through the copper block and out to the vent valve. The vent valve has a micrometer dial which allows precise regulation of the vent aperture size. Control of the flow rate permitted temperature control of the specimen which was located in the evacuated chamber.

The temperature sensor was mounted in the copper block of the cryostat. Temperatures ranging from room temperature to 4.2°K were measured with a platinum resistance sensor model #146 AF2 serial #3520 made by Rosemount Engineering Company. The circuit shown in Figure 2.5 was built to measure the sensor resistance. The basic concept of the circuit is to measure the voltage drop across a known resistance (R_2). In this manner the current in the circuit can be determined. Then measuring the voltage drop across the sensor results in the resistance of the sensor. The resistances (R_2) are shown in Table 2.4. The voltages were read on a Leeds & Northrup 8086 potentiometer, its sensitivity being $\pm 0.05\text{mv}$ resulting in a maximum error of $\pm 2^{\circ}\text{K}$ for the temperature measurement on the platinum sensor. This error is taken into account in the analysis of the results. Both the room temperature and low temperature measurements were



$$\frac{EMF_{GRT}}{EMF_{I MON} / R_2} = R_{RT}$$

TEMP °K	R ₁	R ₂	I MON
1-2	1.5K	10K-196	1mA
2-15	150K	1000-196	.01mA
15-40	15K	100-196	.1mA
40-100	1.5K	10-196	1mA

FIGURE 2.5 TEMPERATURE SENSING CIRCUIT

TABLE 2.4
RESISTANCES (R_2)* IN TEMPERATURE SENSING
CIRCUIT

1.	10,000.02 ohms
2.	1,000.035
3.	100.020
4.	10.009

*As determined on a Fluke Bridge.

made with the sample located in the cryostat. The X-ray tube and recording electronics were turned on and allowed to equilibrate for twenty-four hours before any measurements were made.

Alignment of the specimen in the cryostat was somewhat difficult because the specimen was in vacuum, and not observable through the beryllium window. Prior to use with the cryostat, the diffractometer was aligned as described for the measurement of lattice parameters in section 2.4. A check was then made to assure that the beam would hit approximately the center of the crystal. This was accomplished by wrapping a piece of X-ray film inside two layers of black paper and referencing the top edge of the film with the upper edge of the copper block. With the film taped in place the cryostat was aligned in the X-ray beam. The exposure on the film caused by the X-ray beam could then be compared with the specimen location.

After the preliminary alignment of the cryostat was accomplished the sample was clamped in the cryostat. The crystal was positioned in the center of the beam, aligned parallel to the beam, and adjusted for maximum diffraction intensity as described in section 2.4. The peak 20 was noted for later comparison with the 20 peak at low temperatures.

To record the integrated intensities the 2° slits were used. The 2° slits accepted the entire diffracted beam, and this was checked by removing the 2° slits and

noting that the only change was that which might be expected from the background. The peak was roughly outlined by point counting on either side of the peak. This permitted evaluation of the limits for the peak scan and the locations where the constant background should be read.

The integrated intensity was determined by a continuous scan across the peak, while all of the counts were stored in the digital ratemeter. The total integrated intensity was then displayed visually and recorded on a teletype. The same peak was scanned several times to check that the value was reproducible. Only the highest order peaks were used to obtain the experimental data reported here, but the lower order peaks provided checks on the experiment being done properly. Equation [2.4] shows that high order peaks have a larger M , so that the effect on I is larger for these peaks.

The following procedure was used to cool the cryostat to liquid nitrogen temperatures. The center coolant container and the vent line were flushed with helium gas. After flushing the vent line, a piece of tape was put over the vent exit to keep water vapor from condensing in the line above the micrometer valve. For filling liquid N_2 into either the jacket or the center chamber, it was convenient to use a small styrofoam container with a $3/8$ " diameter stainless steel tube epoxied in the bottom. This provided an insulated funnel that could be filled and left until the cryostat was filled. Once the cryostat was filled the vent could be opened to cool the sample. It took about three hours to cool from room temperature to liquid nitrogen

temperature. When the sample was at liquid nitrogen temperature the alignment procedure discussed above was repeated. This was necessary because thermal contraction caused the sample to move inside the chamber. The intensities were then recorded at liquid N_2 temperature.

The samples studied by this technique and the results from the experiments are discussed in section 3.1. It should be noted that the surfaces of the crystals were abraded with 600 grit silicon carbide paper to minimize the effects of extinction. The intensities were corrected for constant background and for thermal diffuse background by the technique of Skelton and Katz (1969) as discussed in Appendix A.

2.8 Determination of thermal displacements by Flinn's technique

A technique for measuring Debye temperatures has been developed by Flinn (1961) which does not require any assumption about the temperature dependence of the Debye temperature. This technique is based on the measurement of the diffracted intensity at two temperatures as discussed in section 2.6. The equation relating the intensities at two temperatures is simplified if the low temperature approaches zero degrees Kelvin.

The ratio of diffracted intensities at two temperatures was given in equation [2.5]. The Debye-Waller factor (M) can be related to the Debye temperature (θ_D) through equation [1.58] which can be rewritten in the more convenient form:

$$M = \frac{A\sigma^2}{2\theta_M} \left(\frac{\phi(x)}{x} + \frac{1}{4} \right) \quad [2.19]$$

where $A = \frac{6h^2}{mk}$, $\sigma = \frac{\sin\theta}{\lambda}$, and $x = \theta_M/T$.

By substituting equation [2.19] into equation [2.5] the resulting logarithm of the intensity ratio is

$$\begin{aligned} \ln \frac{I(T_2)}{I(T_1)} = & - \frac{A\sigma^2(T_2)}{2\theta_M(T_2)} \left(\frac{\phi(x)}{x} + \frac{1}{4} \right)_{T=T_2} \\ & + \frac{A\sigma^2(T_1)}{2\theta_M(T_1)} \left(\frac{\phi(x)}{x} + \frac{1}{4} \right)_{T=T_1}. \end{aligned} \quad [2.20]$$

By rearranging terms this can be rewritten as

$$\begin{aligned} \ln \frac{I(T_2)}{I(T_1)} = & - \frac{A}{2} \left\{ \frac{\sigma^2(T_2)}{T_2} \left(\frac{\phi(x)}{x} \right)_{T=T_2} - \frac{\sigma^2(T_1)}{T_1} \left(\frac{\phi(x)}{x} \right)_{T=T_1} \right. \\ & \left. + \frac{1}{4} \left(\frac{\sigma^2(T_2)}{\theta_M(T_2)} - \frac{\sigma^2(T_1)}{\theta_M(T_1)} \right) \right\}. \end{aligned} \quad [2.21]$$

The last term in the above equation is nearly zero because neither θ_M or σ change appreciably with temperature. This term is about one percent of the second term at liquid helium temperature, and even less at higher temperatures. The first term approaches zero as the temperature approaches zero. Thus at liquid helium temperature ($T = 4.2^\circ\text{K}$) the first term also can be neglected in comparison to the second

term. Even for temperatures as high as one tenth of the Debye temperature there is only a one percent error in neglecting the first term. This simplification reduces the number of unknowns to one in the equation for the intensity ratio, thus $\theta_M(T_1)$ can be solved directly from the relationship:

$$\ln \frac{I(T_2)}{I(T_1)} = \frac{\Lambda \sigma^2 (T_1) \phi(x) T_1}{\theta_M(T_1)} \quad . \quad [2.22]$$

To solve for $\theta_M(T_1)$ an iterative process is required because $\phi(x)$ is a function of $\theta_M(T_1)$, but the convergence to a value of $\theta_M(T_1)$ is rapid. The computer program for this data reduction is presented in Appendix C.

The experimental techniques for this measurement were basically the same as those discussed in section 2.7, except that He was used as the cooling fluid instead of N_2 . An evacuated transfer tube was used to fill the cryostat with He. The dewar was flushed with room temperature He gas and precooled by keeping the nitrogen cap filled for twelve hours before the transfer. The platinum resistor was only calibrated down to 26°K where the resistance was 11.6 ohm. Unless otherwise reported the resistance was less than one ohm at the experiment temperature, indicating that the temperature was close to 5°K. The results from these experiments are discussed in Chapter III.

2.9 Determination of thermal displacements in partially ordered Cu_3Au

The thermal displacements that are determined by measuring one Bragg peak of an alloy represent an average from both constituents. It is of greater interest to separate the thermal vibrations of the constituents of the alloy. The separation is possible in alloys with some degree of long range order. The formalism for this analysis is presented by Warren (1969). The advantage of Warren's approach is that the results can be adapted to the two temperature technique for measuring the thermal displacements. Although Warren did not apply his development in this manner, this type of measurement allows the thermal displacements to be separated from the static displacements in crystals with less than full long range order. The technique requires the measurement of the Debye-Waller factor for a fundamental and a superlattice peak.

The integrated intensity (I) for Bragg peak is given by

$$I = KFF^* L_p, \quad [2.23]$$

where K is an experimental constant, FF^* is the square of the structure factor, and L_p is the Lorentz polarization factor. For a fundamental reflection where Cu and Au are the A and B atoms respectively:

$$FF^* = 16 \left[x_A (f_A + i\Delta_A) e^{M_A} + x_B (f_B + i\Delta_B) e^{-M_B} \right] \times \left[x_A (f_A - i\Delta_A) e^{-M_A} + x_B (f_B - i\Delta_B) e^{-M_B} \right]. \quad [2.24]$$

In the above equation, x is the composition, and Δ is the imaginary component of the anomalous scattering factor as given by Cromer (1965). The scattering factor f is given by

$$f = f^0 + \Delta f' , \quad [2.25]$$

where f^0 is the standard high energy scattering factor as given by Doyle and Turner (1968) and $\Delta f'$ is the real component of the anomalous scattering factor. After rearranging terms equation [2.24] becomes:

$$FF^* = 16 \left[\left(x_A f_A e^{-M_A} + x_B f_B e^{-M_B} \right)^2 + \left(x_A \Delta_A e^{-M_A} + x_B \Delta_B e^{-M_B} \right)^2 \right] . \quad [2.26]$$

In terms of an average Debye-Waller factor M we can write:

$$M_A = M + \epsilon , \quad M_B = M - \epsilon . \quad [2.27]$$

Since ϵ is small, we can make the approximation $\exp(\epsilon) = 1 + \epsilon$, thus:

$$FF^* = 16 e^{-2M} \left\{ (x_A f_A + x_B f_B)^2 + (x_A \Delta_A + x_B \Delta_B)^2 + [x_B^2 (f_B^2 + \Delta_B^2) - x_A^2 (f_A^2 + \Delta_A^2)] 2\epsilon \right\} . \quad [2.28]$$

With the abbreviation

$$p = \frac{x_B^2 (f_B^2 + \Delta_B^2) - x_A^2 (f_A^2 + \Delta_A^2)}{(x_A f_A + x_B f_B)^2 + (x_A \Delta_A + x_B \Delta_B)^2} , \quad [2.29]$$

and the approximation $1 + 2p\epsilon = \exp[2p\epsilon]$ we obtain:

$$FF^* = 16 [(x_A f_A + x_B f_B)^2 + (x_A \Delta_A + x_B \Delta_B)^2] e^{-2(M-p\epsilon)} . \quad [2.30]$$

For a Cu_3Au superlattice reflection FF^* is given by:

$$\begin{aligned}
 FF^* &= S^2 \left[(f_B + i\Delta_B) e^{-iM_B} - (f_A + i\Delta_A) e^{-iM_A} \right] \times \\
 &\quad \left[(f_B - i\Delta_B) e^{iM_B} - (f_A - i\Delta_A) e^{iM_A} \right] \\
 &= S^2 \left[(f_B e^{-iM_B} - f_A e^{-iM_A})^2 + (\Delta_B e^{-iM_B} - \Delta_A e^{-iM_A})^2 \right]. \quad [2.31]
 \end{aligned}$$

Using equation [2.27] again, we can write

$$\begin{aligned}
 FF^* &= S^2 e^{-2M} \left[(f_B - f_A)^2 + (\Delta_B - \Delta_A)^2 \right. \\
 &\quad \left. + (f_B^2 + \Delta_B^2 - f_A^2 - \Delta_A^2) \right] 2\epsilon. \quad [2.32]
 \end{aligned}$$

Introducing the abbreviation:

$$g = \frac{(f_B^2 + \Delta_B^2) - (f_A^2 + \Delta_A^2)}{(f_B - f_A)^2 + (\Delta_B - \Delta_A)^2}, \quad [2.33]$$

and making the approximation $1 + 2g\epsilon = \exp[2g\epsilon]$ equation [2.32] can be rewritten as:

$$FF^* = S^2 [(f_B - f_A)^2 + (\Delta_B - \Delta_A)^2] e^{-2(M - g\epsilon)}. \quad [2.34]$$

Thus we obtain the result that the Debye-Waller factor as determined in section 2.6 or 2.7 has the form $M - p\epsilon$ for a fundamental reflection and $M - g\epsilon$ for a superlattice reflection. By determining the Debye-Waller factor for a fundamental and a superlattice reflection, M and ϵ can be determined. The thermal displacements of the Cu and Au atoms can then be calculated from M_{Cu} and M_{Au} through equation [2.4].

2.10 Determination of thermal displacements in ordered Cu_3Au crystals by the one temperature technique

The technique in this experiment was basically that used by Chipman (1956). This technique allows determination of the thermal displacements of the individual Cu and Au atoms in fully ordered crystals. The experiment requires measuring fundamental and superlattice integrated intensities for as many reflections as are possible on a crystal face. The intensities are recorded and corrected for constant and thermal diffuse background as discussed in section 2.7.

The equipment used for this type of measurement was the same as discussed in section 2.3 except that: a silver X-ray tube was substituted for the copper tube, a NaI scintillator was the detector, and the crystal was mounted on a goniometer.

The integrated intensity of a fundamental reflection (I_F) for Cu_3Au is given by

$$I_F = K \left(3f_{\text{Cu}} e^{-M_{\text{Cu}}} + f_{\text{Au}} e^{-M_{\text{Au}}} \right)^2 L_p, \quad [2.35]$$

and for a superlattice reflection

$$I_S = K S^2 \left(f_{\text{Au}} e^{-M_{\text{Au}}} - f_{\text{Cu}} e^{-M_{\text{Cu}}} \right)^2 L_p. \quad [2.36]$$

The Lorentz polarization factor (L_p) was defined in equation [2.2]. The M_{Cu} and M_{Au} in these equations contain both the M_{Th} due to thermal vibrations and the M_{St} due to static displacements (Huang distortion). This subject was discussed

in section 2.6. For completely ordered crystals the Huang distortion should be negligible, but for partially ordered crystals the presence of M_{St} has to be considered. The scattering factors f_{Cu} and f_{Au} were corrected for anomalous dispersion with the values of Cromer (1965):

$$\begin{aligned} \Delta f'_{Cu} &= .36 & \Delta_{Cu} &= +.91 \\ \Delta f'_{Au} &= -.90 & \Delta_{Au} &= +6.24 \end{aligned}$$

The values of the high energy scattering factors, f_{Cu}^0 and f_{Au}^0 were taken from the relativistic Hartree-Fock calculation of Doyle and Turner (1968).

By taking the square root of equations [2.35] and [2.36] and then taking sums and differences of these equations:

$$\frac{\sqrt{I_F} - \frac{1}{S} \sqrt{I_S}}{4f_{Cu}\sqrt{L_p}} = \sqrt{K} e^{-M_{Cu}} \quad , \quad [2.37]$$

and

$$\frac{\sqrt{I_F} + \frac{3}{S} \sqrt{I_S}}{4f_{Au}\sqrt{L_p}} = \sqrt{K} e^{-M_{Au}} \quad . \quad [2.38]$$

Except for S , all of the values on the left-hand side of these equations are either measured directly (I_p and I_S) or independently calculated (f , L_p). Values of S were determined by other measurements which were described in section 2.5. Each of the above equations contains the Debye-Waller factor (M) for only one type of atom. M can

be expressed as

$$M = 8\pi^2 \overline{U}_s^{-2} \left(\frac{\sin\theta}{\lambda} \right)^2 = B \left(\frac{\sin\theta}{\lambda} \right)^2 .$$

Taking the logarithm of equations [2.37] and [2.38] results in two equations of the form

$$\ln(L.H.S.) = \ln\sqrt{K} + B \left(\frac{\sin\theta}{\lambda} \right)^2 . \quad [2.39]$$

A graph of the left-hand side of equation [2.39] versus $\left(\frac{\sin\theta}{\lambda} \right)^2$ is a straight-line with a slope of B and an intercept of \sqrt{K} . From the slopes of the lines the thermal displacements of the individual Cu and Au atoms can be determined. Initially the Thomas-Fermi-Dirac scattering factors listed in the International Crystallographic Tables (1955) were used, but these scattering factors would not produce the straight-lines at high $\frac{\sin\theta}{\lambda}$ that are required to measure the thermal displacements. This problem was not encountered once Doyle and Turner's scattering factors were used.

Because this technique results in the sum of the thermal and static displacements, it provides a technique for evaluating the static displacements. As has been noted by Huang (1947) the static displacements result in an effect exactly analogous to thermal displacements. Thus, the resultant displacement determined by this experiment is the sum:

$$\overline{U}_s^{-2} \text{ (thermal)} + \overline{U}_s^{-2} \text{ (static)} .$$

If \overline{U}_s^{-2} (thermal) is then evaluated by the two temperature technique, the difference is the static displacements. The

static displacements in partially ordered Cu_3Au crystals were evaluated by this technique. The results of all the above experiments are discussed in section 3.2.

2.11 Separation of thermal displacements of constituent atoms in disordered alloys

It would be desirable to be able to measure the thermal displacements of the individual constituent atoms in a disordered alloy. This would permit a more realistic evaluation of the vibrational entropy in an alloy. Also, this data would provide more direct information concerning the force fields around individual atoms, rather than the average force field around an average atom. One attempt at separating the individual thermal displacements in disordered alloys has been made by Zviagina and Inveronova (1960). Their analysis requires measuring the diffracted intensity I for two reflections $I(1)$ and $I(2)$ which preferably have significantly different values of $\sin\theta/\lambda$. For a fundamental peak in a FCC solid solution $I(1)$ and $I(2)$ can be expressed as

$$\sqrt{I(1)} = 4\sqrt{K} \left(x_A f_A(1) \exp^{-M_A(1)} + x_B f_B(1) \exp^{-M_B(1)} \right) \times \sqrt{L_p}(1), \quad [2.40]$$

$$\sqrt{I(2)} = 4\sqrt{K} \left(x_A f_A(2) \exp^{-M_A(2)} + x_B f_B(2) \exp^{-M_B(2)} \right) \times \sqrt{L_p}(2) \quad . \quad [2.41]$$

$M(1)$ and $M(2)$ are related to each other through the relationship

$$M_B(2) = M_B(1) \frac{d^2(2)}{d^2(1)}, \quad [2.42]$$

where $d(1)$ and $d(2)$ are the interplanar spacing for the reflection corresponding to $I(1)$ and $I(2)$. After algebraic manipulations of the equations for $I(1)$ and $I(2)$ an equation in terms of known values and $M_A(2)$ is obtained:

$$\sqrt{I(2)} = \left\{ 4\sqrt{K} \sqrt{L_p}(2) x_A f_A(2) \exp^{-M_A(2)} + x_B f_B(2) \right. \\ \left. \left[\frac{\sqrt{I(1)}}{4x_B f_B(1) \sqrt{K} \sqrt{L_p}(1)} - \frac{x_A f_A(1) \exp^{-M_A(2)} \frac{d^2(1)}{d^2(2)}}{x_B f_B(1)} \right] \frac{d^2(2)}{d^2(1)} \right\}. \quad [2.43]$$

The equation for $\sqrt{I(2)}$ cannot be solved analytically for $\exp^{-M_A(2)}$, instead a plot is made of the right-hand side of equation [2.43] as a function of $M_A(2)$. The proper value of $M_A(2)$ is that which gives the experimental value of $\sqrt{I(2)}$.

As is admitted by Zviagina and Inveronova this experiment is difficult to perform with the accuracy necessary to obtain meaningful results. The value for $2B(\text{Au})$ reported by these authors for different sets of reflections varies from 0.8 to 1.2 on an arbitrary scale. This is ± 20 percent from the mean. It would be difficult to make a positive

separation of the A and B displacements with such a variation in one of the constituents. Another difficulty with this experiment is that it only provides a true value of thermal displacements for very dilute alloys and ordered structures close to stoichiometry. At other compositions, such as concentrated solid solutions the Huang scatter due to static displacements also enters into M as determined by this technique.

It was suggested by Dr. L. Skolnick that a separation of thermal displacements might be made with the use of anomalous dispersion. The approach would be to use K_α and K_β radiation close to the absorption edge of one of the constituents of the alloy. An example would be to measure the Debye-Waller factor in a Cu-Au alloy with CuK_α and CuK_β radiation. Because of anomalous dispersion the scattering factor of Cu for CuK_α is different than for CuK_β . But the scattering factor of Au for CuK_α and CuK_β is essentially the same. Because of the difference in scattering factors in Cu it might be possible to take differences of the thermal displacements to isolate the Cu thermal displacements.

Warren (1969) has presented the formalism for analyzing this problem. As was shown in section 2.9, the structure factor for a fundamental reflection from a face centered cubic disordered alloy of composition x_A, x_B is given by

$$F F^* = 16 \left[(x_A f_A + x_B f_B)^2 + (x_{Cu} \Delta_{Cu} + x_{Au} \Delta_{Au})^2 \right] \exp -2M_p .$$

[2.44]

f is the real part of the scattering factor defined by the equation

$$f = f^0 + \Delta f' , \quad [2.45]$$

where f^0 is the scattering factor when the incident radiation has an energy large in comparison to the K absorption edge of the atom. This is the standard scattering factor listed in Doyle and Turner (1968). $\Delta f'$ is the real part of the anomalous dispersion correction, and Δ is the imaginary part of the anomalous correction. M_p is the Debye-Waller factor for a X-ray peak in the alloy. A value of M_p is determined for both the K_α and K_β peaks by the two temperature technique. As shown in section 2.9, M_p is given by

$$M_p = M - p\varepsilon . \quad [2.46]$$

An equation of the form [2.46] results for both the K_α and K_β reflections. The value of p which was defined in equation [2.29] is different for the K_α and K_β radiations because the corrections for anomalous dispersion are different for the two radiations. The two equations for K_α and K_β form two equations with two unknowns i.e. M and ε . Thus M and ε can be determined, and M_A and M_B can be determined from equations [2.27]. The best way to perform this experiment would be to use the two temperature technique with a short wave length radiation. An example would be to study the silver atoms in a silver-gold alloy with $\text{Ag}K_\alpha$ and K_β radiation.

A preliminary calculation was made for a hypothetical Ag-Au solid solution, where the Ag and Au atoms had vibration amplitudes equal to the values in the pure metal. The Debye-Waller factors expected for the K_α and K_β peaks of a (12,0,0) reflection were calculated. The calculation showed that a one percent accuracy in recording the integrated intensities is necessary to be able to differentiate between the values of M_p for the K_α and K_β peaks.

2.12 Summary of experiments to measure thermal displacements

Several types of experiments were used to obtain the reported data. Because of this it will assist in the tabulation of results if each type of experiment is given a number code:

1. These experiments were performed with CuK_α radiation using the two temperature technique at room temperature and liquid nitrogen temperature as described in section 2.7.
2. AgK_α radiation was used with the two temperature technique of Flinn's described in section 2.8. For ordered crystals the analysis of section 2.9 is also applied.
3. AgK_α radiation was used at one temperature as described in section 2.10.

The computer programs to analyze the data for the three above techniques are presented in Appendices B, C, and D respectively.

The experimental error in experiment type one is ± 8 percent; the experimental error in experiments two and three is ± 5 percent in the R.M.S. thermal displacement.

CHAPTER III

RESULTS AND DISCUSSION

3.1 Disordered Cu-Au alloys

The objective of this research was to determine the equilibrium values of the thermal displacements in Cu-Au disordered alloys. The results of this experiment are shown in Table 3.1. To compare this data with the thermal displacements in the literature (presented in Table 1.1) Debye temperatures reported in the literature were converted to thermal displacements using equation [1.65]. The first crystal studied was pure Cu to test experimental techniques. The (220) reflection was used for this study. The result of $.081\text{\AA}$ for the R.M.S. thermal displacement agrees quite well with the values of $.081\text{\AA}$ by Flinn (1960) and $.082\text{\AA}$ by Webb (1962). There have been other values reported such as $.085\text{\AA}$ by Webb (1962), but most of the data clusters around $.081\text{\AA}$. Passaglia (1955) also obtained $.081\text{\AA}$ from data on the electrical resistance Debye temperature of Cu. At the .91Cu-.09Au (a) composition the value of $.090\text{\AA}$ is a little higher than $.086\text{\AA}$ for .92Cu-.08Au by Webb. These two results do agree within the experimental error of $\pm .007\text{\AA}$. Both the .91Cu-.09Au (a) crystal of this work and the .92Cu-.08Au crystal of Webb were annealed at high temperatures and quickly brought to room temperature. Recent work by Cullen (1970) has indicated that months long anneals are necessary to obtain equilibrium in disordered Cu-Au alloys with a high copper concentration. The

TABLE 3.1
EXPERIMENTAL R.M.S. THERMAL DISPLACEMENTS²
IN DISORDERED Cu-Au ALLOYS

Composition	$\left\langle \overline{u_s^2} \right\rangle^{1/2}$	Θ_M °K	a (Å)	Temperature °K
Cu	.081 Å	323.	3.6147	302.
.91Cu-.09Au (b) ³	.082	297.	3.6585	300.
.75Cu-.25Au	.080	266.	3.7488	305.
.2Cu-.8Au	.090	179.	3.9987	301.
Au ¹	.085	175.	4.0783	298.
.91Cu-.09Au (a)	.090	266.	3.6623	301.

1. Owen & Williams Proc. Roy. Soc., A188 509, 1947.
2. All values determined with experiment type one,
see section 2.12, except .91Cu-.09Au(b) which used
experiment type two.
3. Heat treatments a and b are described in Table 2.1.

results for .91Cu-.09Au (b) show that the long time anneal decreased the thermal displacements to $.082\text{\AA}$. Further anneals will be carried out on this crystal to assure that this is the equilibrium value of the thermal displacement.

At the .75Cu-.25Au composition there is still considerable disagreement about the value of the thermal displacements. The result of $.080\text{\AA}$ from this experiment is midway between the values of $.075\text{\AA}$ from Owen and Evans (1967) and $.084\text{\AA}$ from Webb (1962). Both of these values are within the estimated experimental error of $\pm 0.007\text{\AA}$. Webb's samples could have been partially ordered which would explain his high value. Webb reported that he annealed the samples slightly below the solidus and then rapidly cooled them. Possibly this was not sufficiently fast to obtain a completely disordered crystal, and no check of the long range order parameter was reported. Owen and Evans did report evidence of a small undetermined amount of long range order. The result of $.087\text{\AA}$ obtained by Passaglia and Love (1955) from electrical resistivity measurements is in disagreement with this work. Passaglia and Love quenched their samples in water from 550°C ; so they should have been fully disordered. The result of $.121\text{\AA}$ by Bowen (1954) with the same technique and a similar specimen preparation indicates that this technique might not be sensitive to the thermal displacements for this alloy. The results of Cullen (1970) indicated that the data at the .75Cu-.25Au composition did not fit the Grüneisen

relation which was used in the work of both Passaglia and Bowen. In Table 3.2 it is shown that the thermal displacements in the .75Cu-.25Au crystals increase as the crystals are ordered. This increase is due to changes in the vibrational spectrum as will be discussed in section 3.2.

For the .2Cu-.8Au crystal the result of $.090\text{\AA}$ is in agreement with the value of $.088\text{\AA}$ obtained by Passaglia and Love for a .25Cu-.75Au composition. Both of these values are for samples that were given high temperature anneals then cooled to room temperature. Further experiments are being conducted to see if these are true equilibrium values for the thermal displacements.

3.2 Cu₃Au crystals

To compare results reported in the literature for fully ordered Cu₃Au, the thermal displacements were determined for reflections in the [110] direction in reciprocal space on the $S = .98$ crystal. The Ag K_{α} radiation permitted the study of high order reflections out to (880). The results of this study are shown in Figure 3.1. The results for the Cu₃Au crystals are presented in Table 3.3; and in Table 3.4 some of these results are compared with results in the literature. This work agrees with the most recent and probably most accurate work of Gehlen and Cohen (1969). The data of Flinn (1961) is questionable because he did not correct for thermal diffuse scatter, nor were accurate X-ray scattering factors available to him. This will be covered in more detail in the discussion of Chipman's data.

TABLE 3.2
 EXPERIMENTAL R.M.S. THERMAL DISPLACEMENTS
 FOR Cu_3Au DETERMINED FROM (400)
 REFLECTION AS A FUNCTION OF
 THE LONG RANGE ORDER
 PARAMETER (S)

S	$\langle \overline{U_s^2} \rangle^{1/2}$
0.0	.080 Å ¹
0.53	.082
0.80	.084
0.98	.089

1. All values determined with experiment type one.

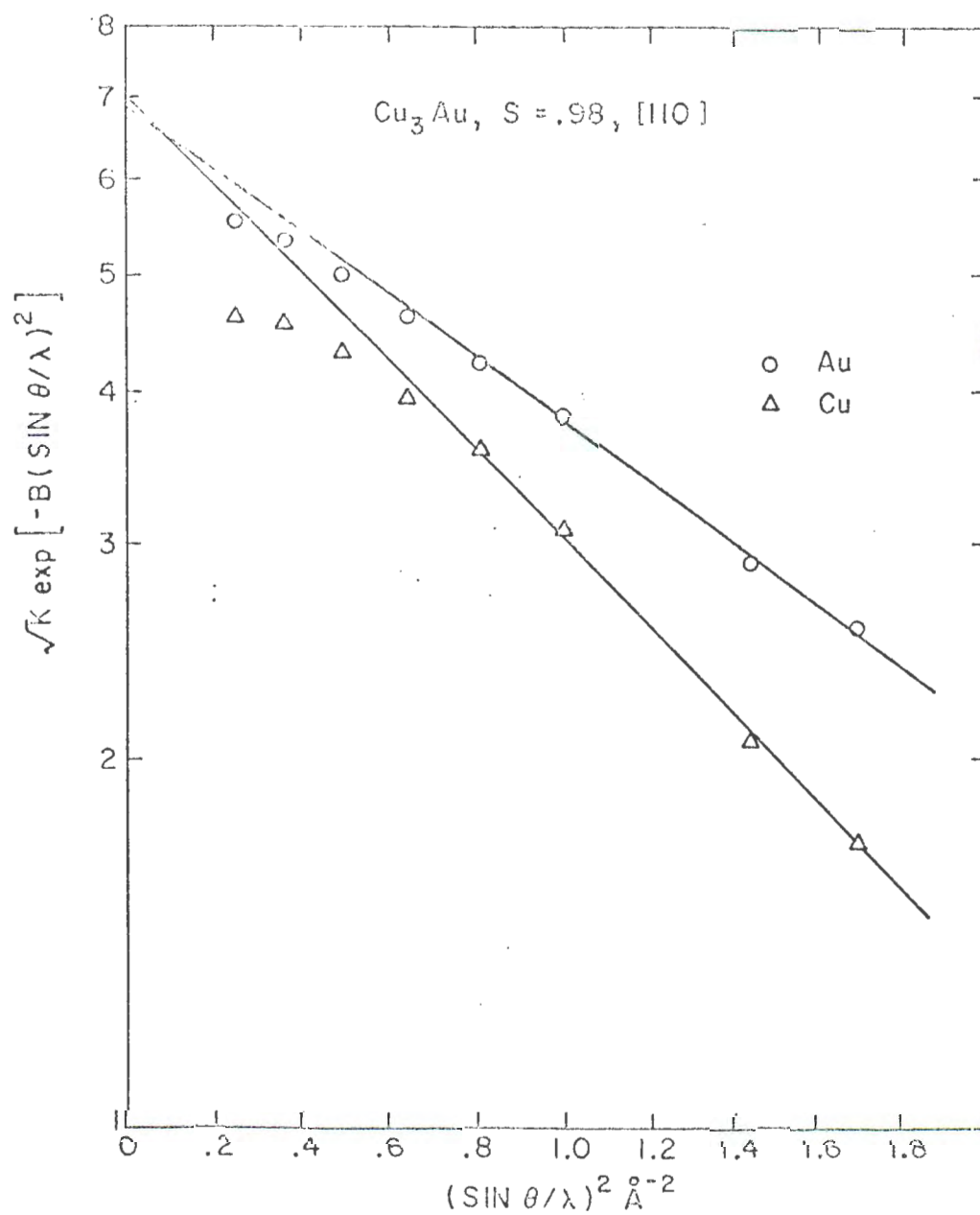


FIGURE 3.1 Z-POL DIFFRACTION DATA FOR Cu_3Au , $S = .98$, $[110]$ DIRECTION.

TABLE 3.3
EXPERIMENTAL R.M.S. THERMAL DISPLACEMENTS OF Cu AND
Au ATOMS IN Cu_3Au AS A FUNCTION OF
THE DEGREE OF LONG RANGE
ORDER (S)

S	$\left\langle \frac{U^2}{S} \right\rangle_{\text{Cu}}^{1/2}$	$\left\langle \frac{U^2}{S} \right\rangle_{\text{Au}}^{1/2}$	Direction [hkl]	Temp. °K	Expt. ¹ Type
.98	.102	.086	110	303.5	3
.98	.088	.088	001	307.0	3
.80	.086	.077	110	299.0	2†
.80	.084	.084	001	302.5	2
.53	.091	.080	110	300.3	2

1. See section 2.12 for explanation of experiment types.

† The low temperature in this experiment was 27°K.

TABLE 3.4
MEASUREMENTS OF R.M.S. THERMAL DISPLACEMENTS
FOR Cu AND Au ATOMS IN Cu_3Au

S	$\langle \overline{u_s^2} \rangle_{\text{Cu}}^{1/2}$	$\langle \overline{u_s^2} \rangle_{\text{Au}}^{1/2}$	$[hkl]$	Experimentor	Temp.
.98	.102	.086	110	Gilmore	303.5
1.00	.099	.084	110	Gehlen	298.0
1.00	.095	.082	110	Schwartz	298.0
.94	.088	.068	110	Flinn	R.T.
.80	.084	.084	001	Gilmore	302.5
.80	.093	.069	001	Chipman	R.T.

A most interesting result was obtained from the thermal displacements in the [001] direction. As shown in Figure 3.2 and Table 3.3, vibration amplitudes of the Cu and Au atoms in this direction are nearly equal, and different from the values in the [110] direction. Lonsdale (1948) points out that for the special case of cubic monatomic crystals the Debye-Waller factor is isotropic. It has also been pointed out by several authors such as Born (1942) and Maradudin *et.al.* (1963) that this simplification is not valid for polyatomic, diatomic or non cubic crystals. Maradudin and Flinn (1963) have shown that it is also not valid to assume that the Debye-Waller factor is isotropic for anharmonic monatomic cubic crystals. Despite these results it is often assumed that the Debye-Waller factor is isotropic in all cubic crystals as is noted by James (1948). This is because it had not been demonstrated experimentally that the thermal vibration amplitudes are anisotropic in diatomic cubic crystals, and the individual thermal displacements in this type of crystal have not been theoretically calculated in different directions.

The only other experimental study reporting the thermal vibrations in the [001] direction is that of Chipman (1956). As shown in Table 3.3, Chipman's results are in disagreement with the present results, but there are several possible reasons for the difference. Chipman did not crystal monochromate his Mo K_{α} radiation; therefore, the background correction is expected to be large in comparison to the weak

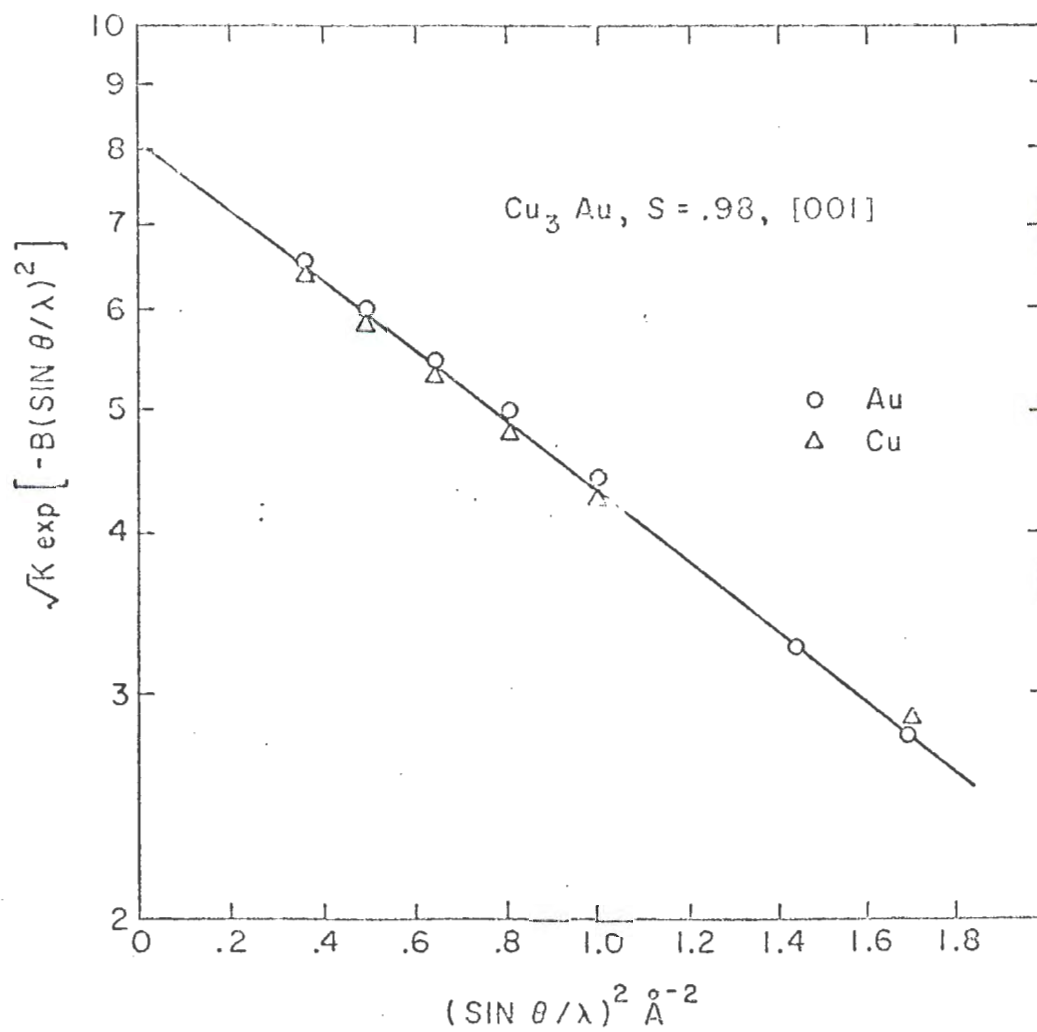


FIGURE 3.2 X-RAY DIFFRACTION DATA FOR Cu_3Au , $S = .98$, $[001]$ DIRECTION

higher order superlattice reflections. Because this was an early experiment, Chipman was not able to correct the Bragg peaks for thermal diffuse scatter (TDS). For high order reflections the TDS intensity is as much as 50 percent of the Bragg peak intensity. Chipman also did not have the use of accurate X-ray scattering factors. The present data for the [001] direction was first analyzed with the scattering factors in the International Tables for X-ray Crystallography (1955), which were used by Chipman. The line for Cu atoms had a large slope at small $\frac{\sin\theta}{\lambda}$, but at larger $\frac{\sin\theta}{\lambda}$ the two curves crossed and then the Au line had a large slope. Changing to the Hartree-Fock scattering factors of Doyle and Turner (1968) eliminated this problem and straight-lines have been obtained at all high values of $\frac{\sin\theta}{\lambda}$. The experimental points do deviate from straight-line behavior at small values of $\frac{\sin\theta}{\lambda}$ due to extinction effects.

The thermal displacements decreased as the degree of long range order was decreased from .98 as shown in Table 3.3. The anisotropy in the thermal displacements is also apparent in the $S = 0.8$ crystal. The difference in the thermal displacements of the $S = .80$ and $S = .53$ crystals is probably not significant. These two results are within the +5 percent accuracy of this technique as quoted by Flinn *et.al.* (1961).

The decrease in thermal displacements corresponds to an increase in the X-ray Debye temperature as the crystal is disordered as shown in Table 3.3. This result appears at first sight to disagree with the results of Flinn (1961) on elastic constant Debye temperatures (θ_E) and Rayne (1957) on specific heat Debye temperatures (θ_D) which, as shown in Table 3.5, decrease with disordering.

At high temperatures the X-ray Debye temperature (θ_M) is related to the inverse second moment of the frequency distribution as shown by Blackman (1955):

$$\frac{1}{\theta_M^2} = \frac{k^2 \frac{1}{3} \int \rho(\nu) \nu^{-2} d\nu}{h^2 \int \rho(\nu) d\nu}.$$

Thus θ_M will be most sensitive to changes in the low frequency end of the distribution. Fukuda (1952) has shown that upon ordering the density of low frequency states increases. This would cause θ_M to decrease upon ordering which agrees with the results of this experiment.

The low temperature specific heat and elastic constant Debye temperatures measured by Flinn and Rayne are related to the inverse third moment of the frequency spectrum. As is pointed out by Herbstein (1961) the low temperature specific heat and elastic constant Debye temperatures are dependent only on the very low frequency vibrations. Because of this, the low temperature θ_D and θ_E are sensitive only to changes at very low frequencies. However, the room temperature X-ray Debye temperature

TABLE 3.5

DEBYE TEMPERATURES FOR ORDERED AND
DISORDERED Cu_3Au CRYSTALS

S	θ_M^1	θ_D^2	θ_E^3
0	266.0	278	281.6
≈ 1.0	241.5	285	283.8

1. Determined from a (400) reflection with experiment type 1, see section 2.12.
2. Rayne (1957).
3. Flinn *et.al.* (1960).

samples more of the frequency spectrum and has a different frequency dependence than θ_D and θ_E , thus it should not be expected that different experiments produce the same result.

The partially ordered crystals were investigated by both the one temperature technique, as presented in Table 3.6 giving the sum of both static and dynamic displacements; and the two temperature technique as presented in Table 3.2 giving only the thermal displacements. The static displacements resulting from the difference in these values for the copper and gold atoms are shown in Table 3.7. Webb (1962) obtained 0.041\AA for the static displacements in Cu_3Au powder samples that were rapidly cooled. Webb's samples should have had a very small amount of long range order, and therefore would be expected to have higher static displacements.

TABLE 3.6

R.M.S. TOTAL DISPLACEMENTS IN PARTIALLY
ORDERED Cu_3Au CRYSTALS

S	$\langle \overline{U_s^2} \rangle^{1/2}_{\text{Cu}}$	$\langle \overline{U_s^2} \rangle^{1/2}_{\text{Au}}$	$[hkl]$	Temp $^{\circ}\text{K}$
.80	.116 Å	.095 Å	110	299.0
.80	.117	.117	001	302.5

TABLE 3.7

R.M.S. STATIC DISPLACEMENTS IN PARTIALLY
ORDERED Cu_3Au CRYSTALS

S	$\langle \overline{U_s^2} \rangle^{1/2}_{\text{Cu}}$	$\langle \overline{U_s^2} \rangle^{1/2}_{\text{Au}}$	$[hkl]$	Temp $^{\circ}\text{K}$
.80	.033 Å	.033 Å	001	302.5
.80	.030	.018	110	299.0

CHAPTER IV

APPLICATION OF EXPERIMENTAL RESULTS TO CELLULAR ALLOY MODEL

4.1 Background

Models of metals and alloys are necessary to develop an understanding of the interaction of atoms and the resulting effect on physical and thermodynamic properties. Complete and rigorous quantum mechanical models for concentrated alloys are not presently available. Approximate models have been developed with the objective of calculating physical and thermodynamic properties. One objective of this approach is to obtain potentials which would be consistent for all properties.

A model for metallic solutions has been developed by Bolsaitis and Skolnick (1968). This model is based on the cellular construction of Wigner and Seitz (1934). The lattice is divided into cells containing an ion core and a negative charge equal to the positive charge on the ion. The cohesive energy (E_{coh}) can then be written as

$$E_{coh} = E_i + E_{el} + E_p \quad [4.1]$$

E_i is the energy necessary to ionize an electron from the gas, and E_{el} is the electronic energy which results from electron-electron and electron-ion interactions. E_p represents pairwise interactions between the ion cores. E_p is

primarily made up of Van der Waals attraction due to the polarizability of the ion cores and exchange repulsion between the ion cores. The Van der Waals attraction (E_{vw}) can be expressed as a sum over the j pairs:

$$E_{vw} = \sum_j - C_{vw}(j) d^{-6}(j), \quad [4.2]$$

where $d(j)$ is the interatomic distance and $C_{vw}(j)$ is a constant which can be calculated from the polarizability of the ions. The exchange repulsion results from the overlap of the closed electron shells of the atoms. This potential is generally represented by a Born-Mayer potential which is an exponential function of distance or by a Lennard-Mie-Jones potential which is a d^{-12} function of distance. Bolsaitis and Skolnick (1968) applied the cellular model to solutions by describing the energy changes through the electron density changes around the constituent atoms. The electron density changes result from changes in electron attracting power which is expressed by an electronegativity scale e.g. the stability ratio proposed by Sanderson (1960). The application of this technique to the electron energies is presented in detail in the paper by Bolsaitis and Skolnick.

The pair energy terms (E_p) entering into the total cohesive energy are dependent upon the local environment of each atom in the alloy. The pair energy will depend upon the types of neighbors, the symmetry, static displacements, and ordering effects. The Van der Waals interaction between the j th pair of atoms was presented in equation [4.2].

$C_{vw}(j)$ is known for the like pairs, and $C_{vw}(j)$ for unlike pairs is zero. E_{vw} is then summed over all pairs, where $d(j)$ is the interatomic distance with static displacements taken into consideration.

The change in the ion exchange interactions on alloying is the most difficult contribution to the energy to evaluate. The exchange energy for the j pair of atoms can be represented by a Born-Mayer potential of the form:

$$E_r = C_j \exp(-A(j) d(j)) \quad [4.3]$$

An estimate of $C(j)$ and $A(j)$ can be made by measuring the pressure derivatives of the elastic constants in Cu-Au alloys as was done by Bolsaitis and Chiarodo (1971). It would be desirable to have other independent checks on the interatomic forces. The thermal displacements of atoms are primarily dependent upon the ion core interactions, and thus will provide an independent check on the interatomic forces.

4.2 Model calculation of thermal displacements

The thermal displacements in the pure copper and gold and in Cu-Au alloys of various compositions were calculated on the basis of pair potential functions as derived from elastic constant and heat of mixing data for alloys of Chiarodo and Bolsaitis (1971). The potentials were developed through the cell model for alloys of Bolsaitis and Skolnick (1968). In order to obtain thermal vibration frequencies and amplitudes from the pairwise potential the

adiabatic approximation (electron energies unaffected by atomic vibrations) was made and an Einstein solid was assumed.

The pairwise potentials ($\phi_p(j)$) used were of the form

$$\phi_p(j) = C(j) \exp [-A(j)d(j)] - C_{vw}(j)d^{-6}(j) \quad , \quad [4.4]$$

where j denotes a particular type of pair, i.e. Cu-Au, Au-Au or Au-Cu. The values of these potential parameters as reported by Bolsaitis and Chiarodo (1971) are listed in Table 4.1. The interatomic distances $d(j)$ are a function of composition and are derived by free energy minimization through relaxation by volume changes on mixing and static displacements. The values of $d(j)$ for the three alloy compositions under consideration here are listed in Table 4.2.

The selection of an Einstein type model for evaluating lattice vibrations and the associated vibrational entropy was made because parallel calculations for the pure metals based on a Born-v.Karman model did not produce an appreciable change in the quantities that were to be calculated. The Einstein model result is compared with a Born-v.Karman calculation developed by Feldman & Horton (1967). Table 4.3 shows that for the same potential the two models calculate the same R.M.S. thermal displacement to within six percent at room temperature. For most calculations that a metallurgical engineer would desire to make, the orders of magnitude increase in difficulty do not justify the small improvement in accuracy of a Born-v.Karman model.

TABLE 4.1
PARAMETERS FOR CELL MODEL POTENTIAL

	$C(j)$ (ergs)	$A(j)_1$ (Å) ⁻¹	$C_{vw}(j)$ ergs(Å) ⁶
Cu-Cu	4.080×10^{-8}	4.79	4.003×10^{-12}
Au-Au	6.869×10^{-7}	5.17	7.606×10^{-11}
Cu-Au	1.529×10^{-7}	4.979	1.745×10^{-11}

TABLE 4.2
INTERATOMIC DISTANCES FROM CELL MODEL

	$d(\text{Cu-Cu})$ Å	$d(\text{Au-Au})$ Å	$d(\text{Au-Cu})$ Å
.91Cu-.09Au	2.559	2.887	2.723
.75Cu-.25Au	2.564	2.892	2.728
.20Cu-.80Au	2.562	2.890	2.726

TABLE 4.3

COMPARISON OF R.M.S. THERMAL DISPLACEMENTS
CALCULATED WITH BORN-V.KARMAN AND
EINSTEIN MODELS AT 298°K

Element	Einstein $\langle \overline{U_s^2} \rangle^{1/2} \text{ \AA}$	Born-v.Karman $\langle \overline{U_s^2} \rangle^{1/2} \text{ \AA}$
Cu	.070	.074
Au	.062	.064

The Einstein model assumes that each atom sets in a cell which is spherically symmetric, and that each atom vibrates independently of the others at an angular frequency ω_E . In pure metals, the force constant for the atom in a cell will be calculated from the pair potentials where all of the neighbors are the same. Then in alloys the force constant is calculated from a geometric average of the force constants of the pure metal and alloy potentials listed in Table 4.1. In a face centered cubic metal each atom at the center of a cell has six pair bonds with the nearest neighbors, and the force constant on the central atom results from the six pairs potentials. The six pair potentials are assumed to be smeared out uniformly over a sphere of 4π steradians. Thus, there are $6/4\pi$ pair "bonds" per steradian. Consider a displacement in the x direction as shown in Figure 4.1. The contribution to the force constant resulting from the pair bonds at angle θ to the x direction in the element of width $r d\theta$ is calculated as follows. The number of steradians in the element θ to $\theta+d\theta$ is given by:

$$\frac{2(r d\theta) 2\pi r \sin\theta}{r^2} \quad .$$

Thus the number of pair bonds in this element is $6 \sin\theta d\theta$. If the force constant due to a pair of atoms is f , then the force constant in the x direction (f_x) is given by

$$f_x = f \cos^2\theta \quad , \quad [4.5]$$

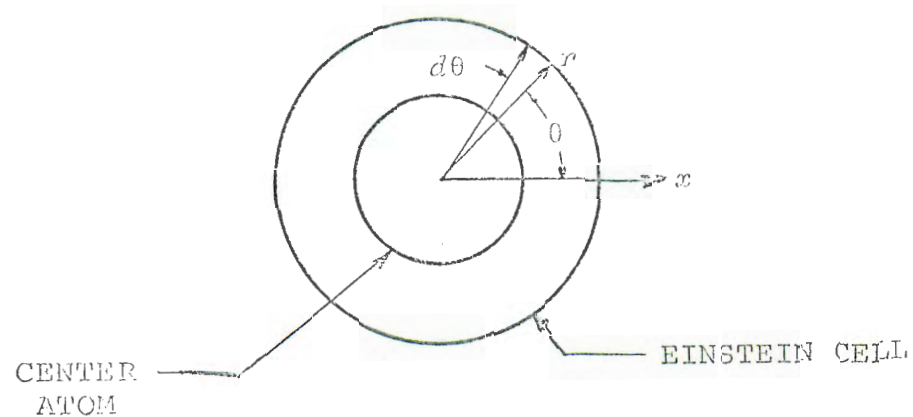


FIGURE 4.1 TWO DIMENSIONAL SCHEMATIC OF
AN EINSTEIN CELL

where the x direction is at an angle θ to the pair bond. The force constant in any direction due to the pair bonds in the element θ to $\theta+d\theta$ is given by $f 6 \sin\theta \cos^2\theta d\theta$.

The force constant on the central atom due to the entire pair density is therefore:

$$FC = \int_0^{\frac{\pi}{2}} f 6 \sin\theta \cos^2\theta d\theta . \quad [4.6]$$

The result of this integration is simply:

$$FC = 2 f . \quad [4.7]$$

The force constant in a particular direction resulting from six pair bonds around an atom is just twice the force of a simple pair bond.

A simple model will now be developed which can be used to relate the thermal displacements with the average force constant in a cell (FC). From classical mechanics the average potential energy (\bar{V}) in the bonds due to a thermal displacement \bar{U}^2 is given by

$$\bar{V} = \frac{1}{2} (FC) (\bar{U}^2) = \frac{3}{2} (FC) (\bar{U}_s^2) . \quad [4.8]$$

The Virial theorem for a harmonic oscillator relates the average total energy (\bar{E}) to the average potential energy (\bar{V}) through the relation:

$$\bar{E} = 2\bar{V} . \quad [4.9]$$

The average energy for a harmonic oscillator in the Einstein model is given by

$$\bar{E} = 3kT \left(\frac{0_{E/T}}{0_{E/T} - 1} \right) , \quad [4.10]$$

where θ_E is the Einstein temperature. In the high temperature limit \bar{E} for a three dimensional harmonic oscillator is given by

$$\bar{E} = 3kT \quad , \quad [4.11]$$

From equation [4.8] in the high temperature limit:

$$\overline{u_s^2} = \frac{kT}{FC} \quad . \quad [4.12]$$

For lower temperatures the result is:

$$\overline{u_s^2} = \frac{\bar{E}}{3(FC)} \quad . \quad [4.13]$$

Assuming the classical high temperature limit and the interatomic distances of Table 4.2 the thermal displacements were calculated from equation [4.12]. The results are in Table 4.4 which shows the experimental displacement; and the calculated values of the thermal displacement, Einstein frequencies and vibrational entropies.

The agreement between measured and calculated displacements in the pure metals seems reasonably good, the 10 to 20 percent discrepancy is most likely ascribable to the simplifying assumptions contained in the model. The change with alloying in calculated thermal displacements at low gold compositions is in agreement with the experimental results for the .91Cu-.09Au (b) crystal. This supports the theory that the increase in thermal displacements observed in the .91Cu-.09Au (a) crystal and in the results of Webb (1962) is a nonequilibrium effect.

TABLE 4.4

EXPERIMENTAL THERMAL DISPLACEMENTS AND LATTICE
PARAMETERS; CALCULATED THERMAL DISPLACEMENTS,
EINSTEIN FREQUENCIES AND VIBRATIONAL
ENTROPIES FOR DISORDERED
Cu-Au ALLOYS

COMPOSITION x_{Au}	LATTICE PARAMETER Å	EXP. $\langle \overline{U_s^2} \rangle^{1/2}$	CALC. $\langle \overline{U_s^2} \rangle^{1/2}$	CALCULATED		$\frac{\Delta S_{\text{vib}}}{\text{Cal.}}$ $\frac{\text{gm-atom}}{^\circ\text{K}}$
				ν_{Cu} 10^{13}sec^{-1}	ν_{Au} 10^{13}sec^{-1}	
0	3.6147	.081 Å	.0677 Å	0.464	---	0
0.09	3.6623 (a)	.090	.0692	0.453	0.267	0.177
	3.6585 (b)	.082				
0.25	3.7488	.080	0.0679	0.458	0.272	0.169
0.30			0.0677	0.458	0.272	0.187
0.70			.0648	0.465	0.281	0.187
0.80	3.9987	.090	.0637	0.469	0.284	0.146
0.90			.0627	0.471	0.287	0.118
1.00	4.0783	.085	.0607	---	0.294	0

1. Heat treatments a and b are described in Table 2.1.

CHAPTER V

CONCLUSIONS

The experimental study of the thermal displacements in the disordered solid solutions revealed that very long anneals were necessary to obtain an equilibrium configuration. Once an equilibrium configuration was achieved, there was a relatively small difference in the thermal vibrations of pure copper and copper rich alloys. There are experiments underway to see if there are similar effects for gold rich alloys.

The changes in thermal vibrations from those of the pure metals were in agreement with the change predicted by a simple Einstein model. The potentials for this model calculation were obtained from the electron cell model of Bolsaitis and Skolnick (1968). Considering the possible experimental uncertainty, the close agreement is remarkable. The magnitude of the calculated and measured values of thermal displacement disagree by 10 to 20 percent. The reason for this is probably due to the assumption that only repulsive ion core and Van der Waals forces were considered in the calculation of thermal displacements. No account was taken of the effect of lattice vibrations on the electron energies. Also long range interaction between atoms was not considered. The Einstein model has been incorporated into the electron cell model for alloys as an approximate method of treating the lattice vibrations. These experiments

provided initial test for the vibrational entropy based upon this version of the Einstein model. Further comparisons with other experimental data will determine if this approach has to be improved, but initial calculations of thermal expansion coefficients has indicated that the Einstein model is useful for calculating thermodynamic properties.

The composition Cu_3Au was investigated to obtain data on the change in vibrational amplitude as a function of degree of order. For the fully ordered Cu_3Au crystal the thermal displacements of the individual Cu and Au atoms were separated by a standard technique for ordered crystals. The results in the [110] direction agree with the most recent and probably most accurate data. The results in the [001] direction show that the vibration amplitude of the Cu atom is not isotropic while that of the Au atom appears to be isotropic. This is the first experimental result which agrees with the analysis by Warren (1969) and others. In partially ordered crystals the individual thermal displacements were separated by an approximate analysis developed by Warren (1969). This analysis was adapted to the determination of Debye-Waller factors by the two temperature technique which allows separation of the thermal and static displacements. This appears to be a valuable technique for the study of partially ordered crystals. It was observed that the X-ray Debye temperature decreases as the

crystal is disordered. This is in agreement with theoretical calculations of Fukuda (1952) for the frequency spectrum in ordered and disordered crystals.

APPENDIX A

THERMAL DIFFUSE SCATTERING CORRECTION

The data recorded was integrated intensities from Bragg reflections. The intensities were corrected for a constant background determined by experiment. The following computer program calculates the ratio of the thermal diffuse to Bragg scattering according to the technique of Skelton and Katz (1969).

A general discussion of the data reduction was given in section 2.6. One of the parameters required to calculate the thermal diffuse scatter is the mean reciprocal square lattice wave velocity (BSUB2). As shown by Skelton *et.al.* BSUB2 ($\langle v^{-2} \rangle$) is given by

$$\langle v^{-2} \rangle = \frac{1}{3} \{ 2\langle v_t \rangle^{-2} + \langle v_l \rangle^{-2} \} , \quad [A.1]$$

where v_t and v_l are the average transverse and longitudinal wave velocities. $\langle v_t \rangle^{-2}$ and $\langle v_l \rangle^{-2}$ have been related to averages of the elastic constants by Anderson (1963) through the expressions

$$\langle v_t \rangle = \sqrt{G_H/\rho} ; \quad \langle v_l \rangle = \sqrt{(K_H + 4G_H/3)/\rho} , \quad [A.2]$$

where G_H and K_H are given by equations [A.3] and [A.4]:

$$G_H = \left\{ \frac{1}{10} \left[\frac{1}{3}(C_{11}+C_{22}+C_{33}) - \frac{1}{3}(C_{12}+C_{23}+C_{31}) \right. \right. \\ \left. \left. + (C_{44}+C_{55}+C_{66}) \right] + \frac{15}{2} \left[4(S_{11}+S_{22}+S_{33}) \right. \right. \\ \left. \left. - 4(S_{12}+S_{23}+S_{13}) + 3(S_{44}+S_{55}+S_{66}) \right]^{-1} \right\} \quad [\text{A.3}]$$

$$K_H = \left\{ \frac{1}{18} \left[(C_{11}+C_{22}+C_{33}) + 2(C_{12}+C_{23}+C_{13}) \right] \right. \\ \left. + \frac{1}{2} \left[(S_{11}+S_{22}+S_{33}) + 2(S_{12}+S_{23}+S_{13}) \right]^{-1} \right\}. \quad [\text{A.4}]$$

For cubic crystals these equations can be simplified because of symmetry and the result is

$$G_H = \frac{1}{10} (C_{11}-C_{12}+3C_{44}) \\ + \frac{15}{2} \left(\frac{12(C_{11}+2C_{12})}{(C_{11}-C_{12})(C_{11}+2C_{12})} + \frac{9}{C_{44}} \right)^{-1} \quad [\text{A.5}]$$

$$K_H = \left(\frac{1}{3} C_{11} + \frac{2}{3} C_{12} \right) \quad [\text{A.6}]$$

The values for C_{11} , C_{12} , and C_{44} listed in Table A.1 were obtained by Chiarodo (1970) for the same crystals as were used for the thermal displacements measurements.

The computer program was written with numerous comment cards to explain notation, input variables, and steps. Because of this, the program should be self-explanatory. The

TABLE A.1
ELASTIC CONSTANTS FOR Cu-Au CRYSTALS
IN 10^{12} DYNES/CM²

CRYSTAL	C_{11}	C_{12}	C_{44}
Cu	1.660	1.189	.755
.91Cu-.09Au	1.716	1.276	.728
.75Cu-.25Au	1.726	1.296	.655
Cu ₃ Au (S = .53)	1.752	1.304	.695
Cu ₃ Au (S = .80)	1.766	1.268	.667
Cu ₃ Au (S = .98)	1.836	1.306	.674
.2Cu-.8Au	1.864	1.532	.481

subroutine for the calculation of the thermal diffuse scattering is further described in Skelton and Katz (1969). Each of the programs in Appendices B, C, and D call this subroutine to correct the integrated intensities.

SUBROUTINE TDSICAL (DENSE,TEMP,WAVLN,BSUBZ,THETA,DETA,DCHI,DEPSI
11,DEPSI2,DONEG1,DONEG2,N,SIGMA1,SIGMA2,ALPHA,ALPHA2)

PROGRAM WILL EVALUATE 1ST ORDER T.D.S. FUNCTION WHEN
GIVEN DETECTOR WINDOW DIMENSIONS AND INTENSITY SCAN

RESULTS GIVE T.D.S./BRAGG SCATTERING RATIO
AS DEFINED IN EQUATION (29).

EQUATION NUMBERS REFER TO T.D.S. PUBLICATION-
ACTA CRYST. XX:YY,1969.

REVISED VERSION WRITTEN 22 DEC. 67

MODIFIED 28 DEC. 67, 29 DEC. 67, 2 JAN. 68, 3 JAN. 68

SECOND REVISED VERSION WRITTEN 4 JAN. 68

MODIFIED 7 JAN. 68

ADAPTED FROM TDSNRL2 ON 12 DEC. 68

SPECIFY DETECTION WINDOW ANGULAR WIDTH (DETA) AND
HEIGHT (UCHI) IN DEGREES
SPECIFY ANGULAR SCAN OF THETA (DEPS11 AND DEPS12)
AND OF OMEGA (DOMEG1 AND DOMEG2), BOTH IN DEGREES
FOR SYMMETRIC SCAN- DEPS11=DEPS12, DOMEG1=DOMEG2

UNDER NORMAL CONDITIONS, SUBROUTINE WILL NOT PRODUCE
OUTPUT. POSSIBLE ERROR MESSAGES WILL BE PRINTED.

NOTATION-

DENSE = MATERIAL DENSITY IN (GMS)/(CM**3)
TEMP = MATERIAL TEMPERATURE IN DEG. KELVIN
WAVLN = X-RAY WAVELENGTH IN CM.
BSUB2 = PLAN RECIPROCAL SQUARE LATTICE WAVE
VELOCITY IN (SEC/CM)**2
THETA = BRAGG ANGLE IN DEGREES
DETA = DETECTOR ANGULAR WIDTH IN DEGREES
UCHI = DETECTOR WINDOW ANGULAR HEIGHT IN DEGREES
DEPS11,DEPS12 = - AND + VALUES OF THETA SCAN
LIMITS IN DEGREES
DOMEG1,DOMEG2 = - AND + VALUES OF OMEGA SCAN
LIMITS IN DEGREES.
N = NO. ITERATIONS IN NUMERICAL INTEG.
SIGMA1,SIGMA2 = - AND + INTEGRATION RESULTS
ALPHA = FINAL TDS/BRAGG SCATTERING RATIO, AS PER
EQ. 29.
ALPHA0 = CONSTANT BACKGROUND INTENSITY
CORRECTION, AS PER EQ. 30.

PI=3.1415927

CON=PI/180.0

BOLTZ=1.38053E-16

CONVERT ALL DEGREES TO RADIANS

DE=DETA*CON

DC=UCHI*CON

E1=DEPS11*CON

E2=DEPS12*CON

O1=DOMEG1*CON

O2=DOMEG2*CON

TT=THETA*CON

DETERMINE CONSTANT FACTOR (EQ. 29)
CON = (6.0*BOLTZ*TEMP*BSUB2)/(DENSE*(WAVLN**3))

2000 CONTINUE

INTEGRATION OVER LOWER REGION (NO. 1)
DEFINE LIMITS OF INTEGRATION (EQ. 31, 32)

DX11=2.0*SQRT ((SIN (TT+E1)**2)+(SIN (TT)**2)-(2.0*SIN (TT+E1)*SIN
1 (TT)*COS (O1-E1)))

ALPHA1=4.0/DX11*SIN (TT)*SIN ((O1-E1)/2.0)
CHECK IF ALPHA1 IS CLOSE TO UNITY

1A1 =ALPHA1

111A1 1200, 1300, 1400, 2000

2000 111A1


```

CALL SJM2(A,B,DE,IC,N,D,D,A2, SGAMMA)
SUM2=SUMC1+ SGAMMA
GO TO 3095
3090 SUM2=SUM1
BKEND2=BKEND1
VOL2=VOL1
3095 ALPHA=COFS *((SUM1+SUM2)*(SIN(TT)**2)
ALPHA2=COFS *((SUM1+SUM2)-(BKEND1+BKEND2))*(SIN(TT)**2)
SIGMA1=SUM1*(SIN(TT)**2)
SIGMA2=SUM2*(SIN(TT)**2)
VOL=VOL1+VOL2
RETURN
9050 FORMAT(24H ALPHA1 CHECK ACTIVATED)
9055 FORMAT(24H ALPHA2 CHECK ACTIVATED)
9060 FORMAT(F20.13,110)
9999 END

```

```

C SUBROUTINE SJM2(ALPHA,BETA,A,B,RSLT)
C SUBROUTINE TO INTEGRATE FUNCTION OF X BETWEEN LOWER
C LIMIT A AND UPPER LIMIT B, USING SIMPSON'S RULE
C ALPHA AND BETA ARE CONSTANT LIMITS IN F-FUNCTION
C INTEGRAL IS DIVIDED INTO N STRIPS
C N MUST BE AN EVEN INTEGER
C
C CHECK IF N IS AN EVEN INTEGER

```

```

1TEST=N-(N/2)*2
IF(1TEST)6010,1010,8010
1010 JEND=N/2-2
FN=N
H=(B-A)/FN
SUM2=0.0
SUM4=0.0
X=A
DO 2010 J=1,JEND
X=X+H
SUM4=SUM4+F(ALPHA,BETA,X)
X=X+H
2010 SUM2=SUM2+F(ALPHA,BETA,X)
X=X+H
SUM4=SUM4+F(ALPHA,BETA,X)
RSLT=H/3.*((F(ALPHA,BETA,A)+F(ALPHA,BETA,B))+4.*SUM4+2.*SUM2)
9999 RETURN
8010 PRINT 9001
RSLT=0.0
GO TO 9999
9001 FORMAT(35HSIMP ERROR-N IS NOT AN EVEN INTEGER)
END

```

```

PRINT 9040,ALPHA1,IA1
BETA1=PI/2.0+TT-PI
GO TO 2005
2003 PRINT 9050
PRINT 9060,ALPHA1,IA1
BETA1=PI/2.0+TT
GO TO 2005
2004 BETA1=PI/2.0+TT-ACOS (ALPHA1)
2005 VOL1=(DE*DC*DX11*5)*N (BETA1)/(4.0*(WAVLN**3))
A1=DX11*SIN (BETA1)
B1=DX11*COS (BETA1)
B1PC=B1*DE
B1MC=B1-DE
C
C      INTEGRATE OVER CHI (I.E. X)
CALL SIMP(A1,B1PC,N,0.0,DC,SCH11)
CALL SIMP(A1,B1MC,N,0.0,DC,SCH12)
SUMCHI=SCH11-SCH12
BKGN1=SUMCHI
C
C      INTEGRATE OVER GAMMA
AAA=1.0/(TAN (BETA1))
CALL SIMP2(AAA,DE,DC,N,0.0,A1,SUMG)
SUM1=SUMCHI+SUMG
C
C      CHECK FOR SYMMETRICAL SCAN
3055 IF(E1-E2) 3060,3055,3060
IF(O1-O2) 3060,3060,3060
C
C      INTEGRATION OVER UPPER REGION (NO. 2)
C      DEFINE LIMITS OF INTEGRATION (Eq. 31, 32)
3060 DX12=2.0*SQRT ((SIN (TT+E2)**2)+(SIN (TT)**2)-(2.0*SIN (TT+E2)*SIN
1 (TT)*COS (O2-E2)))
ALPHA2=4.0/DA12*SIN (TT)*SIN (O2-E2)/2.0
C
C      CHECK IF ALPHA2 IS CLOSE TO UNITY
IA2 =ALPHA2
IF(IA2 )2016,2014,2013
2016 PRINT 9055
PRINT 9060,ALPHA2,IA2
BETA2=PI/2.0+TT-PI
GO TO 2015
2013 PRINT 9055
PRINT 9060,ALPHA2,IA2
BETA2=PI/2.0+TT
GO TO 2015
2014 BETA2=PI/2.0+TT-ACOS (ALPHA2)
2015 VOL2=(DE*DC*DX11*5)*N (BETA2)/(4.0*(WAVLN**3))
A2=DX12*SIN (BETA2)
B2=DX12*COS (BETA2)
B2PC=B2*DE
B2MC=B2-DE
C
C      INTEGRATE OVER CHI (I.E. X)
CALL SIMP(A2,B2PC,N,0.0,DC,SCH11)
CALL SIMP(A2,B2MC,N,0.0,DC,SCH12)
SUMCH2=SCH11-SCH12
BKGN2=SUMCH2
C
C      INTEGRATE OVER GAMMA
AAA=1.0/(TAN (BETA2))

```

```

FUNCTION F(ALPHA,BE11,X)
Z=SQRT(ALPHA**2+X**2)
F=ALPHA//*ATAN(BE11/Z)
RETURN
END

```

```

C SUBROUTINE SIMP2(AA1,A1A,A2A,B,A,B,PSLT)
C SUBROUTINE TO INTEGRATE FUNCTION OF X BETWEEN LOWER
C LIMIT A AND UPPER LIMIT B, USING SIMPSON'S RULE
C QUANTITIES A AND B IN F(A,B,X) MAY BE VARIABLES
C OF THE INTEGRATION
C MODIFIED 29 DEC. 67
C RENNOFFED 4 JAN. 66
C INTEGRAL IS DIVIDED INTO N STRIPS
C N MUST BE AN EVEN INTEGER
C
C CHECK IF N IS AN EVEN INTEGER

```

```

      ITEST=N-(N/2)*2
      IF (ITEST)5010,1010,6010
1010 JEND=N/2-2
      FN=N
      H=(B-A)/FN
      SUM2=0.0
      SUM4=0.0
      X=A
      DO 2010 J=1,JEND
      X=X+H
      SUM4=SUM4+F(A2A,X*AAA+A1A,X)-F(A2A,X*AAA-A1A,X)+
1G(A1A,X*AAA+A1A,A2A,X)-G(-A1A,X*AAA-A1A,A2A,X)
      X=X+H
2010 SUM2=SUM2+F(A2A,X*AAA+A1A,X)-F(A2A,X*AAA-A1A,X)+
      1G(A1A,X*AAA+A1A,A2A,X)-G(-A1A,X*AAA-A1A,A2A,X)
      X=X+H
      SUM4=SUM4+F(A2A,X*AAA+A1A,X)-F(A2A,X*AAA-A1A,X)+

```

```

1G(A1A,X*AAA+A1A,A2A,X)-G(-A1A,X*AAA-A1A,A2A,X)
      FFA=F(A2A,A*AAA+A1A,A)-F(A2A,A*AAA-A1A,A)+
1G(A1A,A*AAA+A1A,A2A,A)-G(-A1A,A*AAA-A1A,A2A,A)
      FFB=F(A2A,B*AAA+A1A,B)-F(A2A,B*AAA-A1A,B)+
1G(A1A,B*AAA+A1A,A2A,B)-G(-A1A,B*AAA-A1A,A2A,B)
      RSLT=H/3.0*(FFA+FFB+4.0*SUM4+2.0*SUM2)
9999 RETURN
8010 PRINT 9001
      RSLT=D.0
      GO TO 9999
9001 FORMAT(30HSTEP2 ERROR-N IS NOT AN EVEN INTEGER)
      END

```

```

FUNCTION G(F,H,C,X)
Z=SQRT(F**2+X**2)
G=H//*ATAN(C/Z)
RETURN
END

```

APPENDIX B

COMPUTER PROGRAM FOR DETERMINATION OF THERMAL
DISPLACEMENTS BY THE TWO TEMPERATURE
TECHNIQUE AT ROOM AND LIQUID
NITROGEN TEMPERATURES

The following computer program analyzes the data as discussed in section 2.6. The results of the analysis are the Debye temperatures at room and liquid nitrogen temperature, the Debye-Waller factor (M) at room temperature for the reflection being considered, and the thermal displacements at room temperature.

```

DIMENSION DT(2,100),T(2),D(2),B(2),CT(2),X(2,100),PSI(2,100),
1  S(100),DENSE(2),P(2)
HK=6.626*10.C**(-27)/(1.381*10.**(-16))
H=6.676*10.**(-27)
3 READ(1,4)X1,L
C X1 IS A COMPONENT CONCENTRATION
4 FORMAT(1F5.0,111)
C IF L=1 ANOTHER SET OF DATA FOLLOWS
X2=1.-X1
C X2 IS B COMPONENT CONCENTRATION
WRITE(6,25)
25 FORMAT(1H ,7X,3HX1 ,7X,3HX2 )
WRITE(6,22) X1,X2
22 FOR 1AT(1H1,2F10.3)
READ(5,5)G1,G2,ALP1,ALP2,AM1,AM2
5 FORMAT(2F10.0,4F10.0)
C G1 IS GRUNEISEN PARAMETER FOR A
C G2 IS GRUNEISEN PARAMETER FOR B
G=X1*G1+X2*G2
ALP=X1*ALP1+X2*ALP2
C ALP1 IS LINEAR EXPANSION COEFFICIENT FOR A
C ALP2 IS LINEAR EXPANSION COEFFICIENT FOR B
AM= AM1*X1+X2*AM2
C AM1 IS ATOMIC MASS OF A IN GM/ATOM
C AM2 IS ATOMIC MASS OF B IN GM/ATOM
WRITE(6,26)
26 FORMAT(1H ,14X,2H3 ,13X,3HALP ,12X,1HAM)
WRITE(6,20) G,ALP,AM

```

```

20 FORMAT(1H0,1F16.2,2E16.4)
   READ(5,2) DT(1,1),P1,P2,T(1),T(2),D(1)

   2 FORMAT(3F10.0,1E10.0)
C  DT(1,1) IS AN ASSUMED DEBYE TEMPERATURE FOR A AT T(1). DT(1,1) IS LATER
C  SELF CONSISTENTLY CALCULATED FOR USE IN CALCULATING THERMAL DISPLACEMENTS
C  P1 IS INTEGRATED INTENSITY AT TEMPERATURE T(1)
   D(2)=D(1)-D(1)*ALP*(T(1)-T(2))
C  P2 IS INTEGRATED INTENSITY AT TEMPERATURE T(2)
C  D(1) IS THE INTERPLANAR DISTANCE FOR THE HKL PLANES AT T(1)
C  D(2) IS THE INTERPLANAR DISTANCE FOR THE HKL PLANES AT T(2)

   WRITE(6,27)
27 FORMAT(1H ,9H DT(1,1) ,8X,2HP1,8X,2HP2 ,5X,5HT(1) ,5X,5HT(2) ,5X,
15HD(1) ,5X,5HD(2) )
   WRITE(6,21) DT(1,1),P1,P2,T(1),T(2),D(1),D(2)
21 FORMAT(1H0,5F10.1,2E10.4)

   DETA=2.0
C                                     DETA = DETECTOR ANGULAR WIDTH IN DEGREES
   DCHI=3.5
C                                     DCHI = DETECTOR WINDOW ANGULAR HEIGHT IN DEGREES
   N=500
C                                     N = NO. ITERATIONS IN NUMERICAL INTEG.
   WAVLN=1.54051*10.**(-8)
C                                     WAVLN = X-RAY WAVELENGTH IN CM.
   READ(5,6)DEPS11,DENSE(1),THETA,C11,C12,C44
   6 FORMAT(3F10.0,3E10.0)
   WRITE(6,31)
31 FORMAT(1H ,4X,6H THETA,4X,6HDEPS11,6X,4HDETA,6X,4HDCHI)
   WRITE(6,32) THETA,DEPS11,DLTA,DCHI
32 FORMAT(1H ,4F10.4)
C                                     DEPS11,DLTA,DCHI = - 1/N + 1/V = 1/N OF THETA SCAN

```



```

C                               LIMITS IN DEGREES
C
C      DENSE = MATERIAL DENSITY IN (GMS)/(CM**3)
C      THETA = BRAGG ANGLE IN DEGREES
C      BSUB2  = MEAN RECIPROCAL SQUARE LATTICE WAVE
C              VELOCITY IN (SEC/CM)**2
C
C      C11,C12,C44 ARE EXPERIMENTALLY DETERMINED ELASTIC CONSTANTS
C
C      DEPSI2=DEPSI1
C      DOMEQ1=DEPSI1
C      DOMEQ2=DOMEQ1
C      FOR SYMMETRIC SCAN- DEPSI1=DEPSI2, DOMEQ1=DOMEQ2
C
C      P(1)=P1
C      P(2)=P2
C      DENSE(2)=DENSE(1)/(1.-3.*ALP*(T(1)-T(2)))
C      DO 14 M=1,2
C      TEMP=T(M)
C      TEMP = MATERIAL TEMPERATURE IN DEG. KELVIN
C
C      DENS =DENSE(M)
C      GH=((C11-C12+3.*C44)/10.+15.*((12.*(C11+2.*C12)/((C11-C12)*(C11+2.
1      *(12))+9./C44)**(-1))/2.)
C      FH=(C11/3.+(2.*C12)/3.)
C      VT=SQRT(GH/DENS)
C      VL=SQRT((FH+4.*GH/3.)/DENS)
C      BSUB2=(2.* VT**(-2)+VL**(-2))/3.
C      WRITE(6,33)
33  FORMAT(1H ,11X,5HWAVLN,13X,3HC11,13X,3HC12,13X,3HC44 ,11X,5HBSUB2)
C      WRITE(6,34) WAVLN,C11,C12,C44,BSUB2
34  FORMAT(1H ,5E16.4)
C      CALL IDSCAL (DENS ,TEMP,WAVLN,BSUB2 ,THETA,DETA,DCHI,DEPSI1,DEPS
112,100 ,100,100,100 , SIGMA1,SIGMA2,ALPHA,ALPHA2 )
C      WRITE(6,35)

```

```

30 FORMAT(1H ,9X,7HALPHAB )
   WRITE(6,74)ALPHAB
74 FORMAT(1H0,1F16.4)
C ALPHAB IS THE TDS TO BRAGG INTENSITY RATIO IF A CONSTANT BACKGROUND
C CORRECTION TO THE DATA HAS BEEN MADE
   P(M)=I(M)/(1.+ALPHAB)
C THIS STEP CORRECTED THE INTENSITIES FOR TDS BACKGROUND
14 CONTINUE
   P1=P(1)
   P2=P(2)
   WRITE(6,28)
28 FORMAT(1H ,8X,2HP1,8X,2HP2,3X,13HTDS CORRECTED )
   WRITE(6,24)P1,P2
24 FORMAT(1H0,2F10.0)
   Y=(ALOG(P1/P2))*0.5*(-1.0)
C Y IS M(T1)-M(T2) FROM EQ 3 SECTION 2.6
   HAM=H/AM
   A=6.*HK*HAM
   PI=3.14159
   DO 11 I=1,2
   B(I)=T(I)/(4.*4(I)**2)
   CT(I)=1./(16.*D(I)**2)
11 CONTINUE
   GRUN=(1.+3.*ALP*G*(T(1)-T(2)))
C GRUN IS THE GRUNEISEN CORRECTION TO THE DEBYE TEMPERATURE
   DO 12 J=1,100
C THIS DO LOOP STARTS A SELF CONSISTENT CALCULATION OF DT
   DT(2,J)=DT(1,J)*GRUN
   DELTA=CT(1)/DT(1,J)-CT(2)/DT(2,J)
   DO 13 I=1,2

```

```

      X(1,J)=DT(1,J)/T(1)
      PSI(1,J)=1.-X(1,J)/4.+X(1,J)**2/36.-X(1,J)**4/3600.
C   PSI COMES FROM EQ. 5.95 JAMES (1948)
      13 CONTINUE
      S(J)=B(1)*PSI(1,J)-(B(2)*PSI(2,J))/GRUN**2
      K=J+1
      DT(1,K)=(S(J)/(Y/A-DELTA))**0.5
C   DT(1,K) IS THE CALCULATION OF THE NEW DEBYE TEMPERATURE AS IN EQ 7 SECT 2.6
      DIFF=ABS(DT(1,J)-DT(1,K))
      IF(DIFF.LT.0.1) GO TO 10
      12 CONTINUE
      10 DT(2,K)=DT(1,K)*GRUN
      DWF=A*((B(1)*PSI(1,J)/DT(1,K))+CT(1))/DT(1,K)
C   DWF IS THE DEBYE-WALLER FACTOR NOTED IN JAMES AS 'M'.
      USSQ=3.*HK*HAM*T(1)*(PSI(1,J)+X(1,J)*0.25)/(4.0*PI**2*DT(1,K)**2)
C   USSQ IS THE MEAN SQUARE THERMAL DISPLACEMENT CALCULATED AS IN EQ. 4 SECT 2.6
      U=USSQ**0.5
      WRITE(6,29)
      29 FORMAT(1H ,2X,6HDT(1,K) ,2X,6HDT(2,K) ,5X,5HDIFF ,2X,2HU ,12X,
     1 4HDWF ,11X,5HUSSQ ,14X,2HU )
      WRITE(6,23) DT(1,K),DT(2,K),DIFF,J,DWF,USSQ,U
      23 FORMAT(1H0,3F10.1,114,3E16.4)
      IF(L.EQ.1) GO TO 3
      STOP
      END

```

APPENDIX C

COMPUTER PROGRAM TO DETERMINE THERMAL
DISPLACEMENTS BY FLINN'S TECHNIQUE

The following computer program analyzes the data at room and liquid helium temperatures as discussed in section 2.7. The results of the analysis are the Debye temperature Debye-Waller factor and thermal displacements at room temperature.

```

1  DIMENSION DT(2,100),T(2),D(2),B(2),CT(2),X(2,100),PSI(2,100),
    DENSE(2),P(2)
    G=0.0
    HK=6.626*10.0**(-27)/(1.381*10.0**(-16))
    H=6.626*10.0**(-27)
3  READ(5,4)X1,L
C  X1 IS A COMPONENT CONCENTRATION
4  FORMAT(1F5.0,111)
C IF L=1 ANOTHER SET OF DATA FOLLOWS
    X2=1.-X1
C  X2 IS B COMPONENT CONCENTRATION

```

```

25 WRITE(6,25)
   FORMAT(1H,7X,3HX1,7X,3HX2)
   WRITE(6,22) A1,X2
22 FORMAT(1H1,2F10.3)
   READ(5,5)G1,G2,ALP1,ALP2,AM1,AM2
5 FORMAT(2F10.0,4E10.0)
   ALP=X1*ALP1+X2*ALP2
C ALP1 IS LINEAR EXPANSION COEFFICIENT FOR A
C ALP2 IS LINEAR EXPANSION COEFFICIENT FOR B
   AM=AM1*X1+X2*AM2
C AM1 IS ATOMIC MASS OF A IN GM/ATOM
C AM2 IS ATOMIC MASS OF B IN GM/ATOM
   WRITE(6,26)
26 FORMAT(1H,14X,2HG,13X,3HALP,13X,2HAM)
   WRITE(6,20) G,ALP,AM
20 FORMAT(1H0,1F16.2,2E16.4)
   READ(5,2) DT(1,1),P1,P2,T(1),T(2),D(1)
2 FORMAT(5F10.0,1E10.0)
C DT(1,1) IS AN ASSUMED DEBYE TEMPERATURE FOR A AT T(1). DT(1,1) IS LATER
C SELF CONSISTENTLY CALCULATED FOR USE IN CALCULATING THERMAL DISPLACEMENTS
C P1 IS INTEGRATED INTENSITY AT TEMPERATURE T(1)
C P2 IS INTEGRATED INTENSITY AT TEMPERATURE T(2)
C D(1) IS THE INTERPLANAR DISTANCE FOR THE HKL PLANES AT T(1)
   WRITE(6,27)
27 FORMAT(1H,9H,DT(1,1),8X,2HP1,8X,2HP2,5X,5HT(1),5X,5HT(2),5X,
15HD(1),5X,5HD(2))
   WRITE(6,21) DT(1,1),P1,P2,T(1),T(2),D(1),D(2)
21 FORMAT(1H0,5F10.1,2E10.4)
   DETA=2.0
C DETA = DETECTOR ANGULAR WIDTH IN DEGREES
   DCHI=3.5
C DCHI = DETECTOR WINDOW ANGULAR HEIGHT IN DEGREES
   N=500
C N = NO. ITERATIONS IN NUMERICAL INTEG.
   WAVLN=.561*10.**(-8)
C WAVLN = X-RAY WAVELENGTH IN CM.
   READ(5,6)DEPS11,DENSE(1),THETA,C11,C12,C44
6 FORMAT(3F10.0,3E10.0)
   WRITE(6,31)
31 FORMAT(1H,4X,6H THETA,4X,6HDEPS11,6X,4HDETA,6X,4HDCHI)
   WRITE(6,32) THETA,DEPS11,DETA,DCHI
32 FORMAT(1H,4F10.4)
C DEPS11,DEPS12 = - AND + VALUES OF THETA SCAN
C LIMITS IN DEGREES
C DENSE = MATERIAL DENSITY IN (GMS)/(CM**3)
C THETA = BRAGG ANGLE IN DEGREES
C BSUB2 = MEAN RECIPROCAL SQUARE LATTICE WAVE
C VELOCITY IN (SEC/CM)**2
C C11,C12,C44 ARE EXPERIMENTALLY DETERMINED ELASTIC CONSTANTS
   DEPS12=DEPS11
   DOME1=DEPS11
   DOME2=DOME1
C FOR SYMMETRIC SCAN= DEPS11=DEPS12, DOME1=DOME2
   P(1)=P1
   P(2)=P2
   DENSL(2)=DENSE(1)/(1.-3.*ALP*(T(1)-T(2)))
   DO 14 M=1,2

```



```

C      TEMP=T(M)      TEMP = MATERIAL TEMPERATURE IN DEG° KELVIN
      DENS=DENSE(M)
      GH=((C11-C12+3.*C44)/10.+15.*((12.*(C11+2.*C12)/(C11-C12)*(C11+2.
1      *C12))+9./C44)*(-1))/2.)
      FH=(C11/3.+(2.*C12)/3.)
      VT=SQRT(GH/DENS)
      VL=SQRT((FH+4.*GH/3.)/DENS)
      BSUB2=(2.*VT*(-2)+VL*(-2))/3.
      WRITE(6,33)
33  FORMAT(1H,11X,5H,WAVLN,13X,3HC11,13X,3HC12,13X,3HC44,11X,5HBSUB2)
      WRITE(6,34) WAVLN,C11,C12,C44,BSUB2
34  FORMAT(1H,5E16.4)
      CALL TDSCL (DENS,TEMP,WAVLN,BSUB2,THETA,DETA,DCH1,DEPS1,DEPS
112'DOMEG1'DOMEG2'N,SIGMA1'SIGMA2'ALPHA'ALPHAB)
      WRITE(6,30)
30  FORMAT(1H,9X,7HALPHAB)
      WRITE(6,74)ALPHAB
74  FORMAT(1H0,1F16.4)
C  ALPHAB IS THE TDS TO BRAGG INTENSITY RATIO IF A CONSTANT BACKGROUND
C  CORRECTION TO THE DATA HAS BEEN MADE
      P(M)=P(M)/(1.+ALPHAB)
C  THIS STEP CORRECTED THE INTENSITYS FOR TDS BACKGROUND
14  CONTINUE
      P1=P(1)
      P2=P(2)
      WRITE(6,28)
28  FORMAT(1H,8X,2HP1,8X,2HP2,3X,13HTDS CORRECTED)
      WRITE(6,24)P1,P2
24  FORMAT(1H0,2F10.0)
      Y=(ALOG(P1/P2))*0.5*(-1.0)
C  Y IS H(T1)-H(T2) FROM EQ 3 SECTION 2.6
      HAM=H/AM
      A=6.*HK*HAM
      I=1
      B(I)=T(1)/(4.*D(1)**2)
      CT(I)=1./(16.*D(1)**2)
      P1=3.14159
      DO 12 J=1,10
C  THIS DO LOOP STARTS A SELF CONSISTENT CALCULATION OF DT
      X(1,J)=DT(1,J)/T(1)
      PSI(1,J)=1.-X(1,J)/4.+X(1,J)**2/36.-X(1,J)**4/3600.
C  PSI COMES FROM EQ.5.95 JAMES(1948)
      K=J+1
      DT(1,K)=SQRT(A*PSI(1,J)*T(1)/(Y+4.*D(1)**2))
C  DT(1,K) IS THE CALCULATION OF THE NEW DEBYE TEMPERATURE AS IN EQ 7 SECT 2.6
      DIFF=ABS(DT(1,J)-DT(1,K))
      IF(DIFF.LT.0.1) GO TO 10
12  CONTINUE
10  DWF=A*((H(1)*PSI(1,J)/DT(1,K))+CT(1))/DT(1,K)
C  DWF IS THE DEBYE-WALLER FACTOR NOTED IN JAMES AS 'M'
      USSQ=3.*HK*HAM*T(1)*(PSI(1,J)+X(1,J)*0.25)/(4.0*P1**2*DT(1,K)**2)
C  USSQ IS THE MEAN SQUARE THERMAL DISPLACEMENT CALCULATED AS IN EQ. 4 SECT 2.6
      U=USSQ**0.5
      WRITE(6,29)
29  FORMAT(1H,2X,8HDT(1,K),2X,8HDT(2,K),5X,5HDIFF,2X,2HU,12X,
1 4HDWF,11X,5HUSSQ,14X,2HU)

```

```
23 WRITE(6,23) DT(1,K),DT(2,K),DIFF,J,DWF,USSQ,U  
   FORMAT(1H0,3F10.1,114,3E16.4)  
   IF(L.EQ.1) GO TO 3  
   STOP  
   END
```

APPENDIX D

COMPUTER PROGRAM TO CORRECT INTEGRATED
INTENSITIES FOR THERMAL
DIFFUSE SCATTER

This computer program corrects the integrated intensities for thermal diffuse scattering. The results of this program are then used in the analysis of the long range order parameter in section 2.5 or in the analysis of thermal displacements as in section 2.10.

```

C      N=500                      N      = NO. ITERATIONS IN NUMERICAL INTEG.
C      DELTA=2.0                  DELTA = DETECTOR ANGULAR WIDTH IN DEGREES
C      DCHI=3.5                   DCHI = DETECTOR WINDOW ANGULAR HEIGHT IN DEGREES
C      WAVLN=0.561*10**(-8)       WAVLN = X-RAY WAVELENGTH IN CM.
C      READ(5,1) DENS,C11,C12,C44
C      1 FORMAT(1F10.0,3E10.0)    DENS = MATERIAL DENSITY IN (GMS)/(CM**3)
C      C11,C12,C44 ARE EXPERIMENTALLY DETERMINED ELASTIC CONSTANTS
C      WRITE(6,8)
C      8 FORMAT(1H1,6X,4H DENS,13X,3HC11,13X,3HC12,13X,3HC44)
C      WRITE(6,34) DENS,C11,C12,C44
C      34 FORMAT(1H,4E16.4)
C      GH=((C11-C12+3.*C44)/10.+15.*((12.*(C11+2.*C12)/((C11-C12)*(C11+2.
C      *C12))+9./C44))*(-1))/2.)
C      1
C      FH=(C11/3.+(2.*C12)/3.)
C      VL=SQRT((FH+4.*GH/3.)/DENS)
C      VT=SQRT(GH/DENS)
C      BSUB2=(2.* VT**(-2)+VL**(-2))/3.
C      3 READ(5,2) PB,DEPS11, THETA,TEMP,L
C      2 FORMAT(4F10.0,111)
C      PB IS INTEGRATED INTENSITY AT TEMPERATURE T(1) BEFORE TDS CORRECTION
C      DEPS11,DEPS12 = - AND + VALUES OF THETA SCAN
C      LIMITS IN DEGREES
C      THETA = BRAGG ANGLE IN DEGREES
C      BSUB2 = MEAN RECIPROCAL SQUARE LATTICE WAVE
C      VELOCITY IN (SEC/CM)**2
C      DEPS12=DEPS11
C      DOMEGL=DOMEGL
C      DOMEGL=DOMEGL
C      FOR SYMMETRIC SCAN= DEPS11=DEPS12, DOMEGL=DOMEGL2
C      TEMP = MATERIAL TEMPERATURE IN DEG. KELVIN
C      WRITE(6,5)
C      5 FORMAT(1H1,4X,2HPB,6X,6HDEPS11,2X,3X,5H THETA,5X,4HTEMP,8X,5HBSUB2)
C      WRITE(6,4) PB,DEPS11,THETA,TEMP,BSUB2
C      4 FORMAT(1H,4F10.2,1E16.4)
C      CALL TDSCAL (DENS,TEMP,WAVLN,BSUB2,THETA,DELTA,DCHI,DEPS11,DEPS
C      112,DOMEGL,DOMEGL2,N,SIGMA1,SIGMA2,ALPHA,ALPHAB)
C      WRITE(6,30)
C      30 FORMAT(1H,9X,7HALPHAB)
C      WRITE(6,74) ALPHAB
C      74 FORMAT(1H0,1E16.4)
C      ALPHAB IS THE TDS TO BRAGG INTENSITY RATIO IF A CONSTANT BACKGROUND
C      PA =PB / (1.+ALPHAB)
C      PA IS INTEGRATED INTENSITY AT TEMPERATURE T(1) AFTER TDS CORRECTION
C      THIS STEP CORRECTED THE INTENSITIES FOR TDS BACKGROUND
C      WRITE(6,7)
C      7 FORMAT(1H0,4X,2HPA)
C      WRITE(6,6) PA
C      6 FORMAT(1H,1F10.0)
C      IF(L.EQ.1) GO TO 3
C      IF L=1 ANOTHER SET OF DATA FOLLOWS
C      STOP
C      END

```

APPENDIX E
SAMPLE DATA OUTPUT

The following data is an example of the output data from this experiment. The data was for a Cu_3Au crystal which upon final analysis had a long range order parameter of $S = .80$. This data is for a $[100]$ direction and the reflection is indicated over each set of data. Copper K_α radiation was used in this experiment. First the background count rate was determined on either side of the peak by counting for 100 seconds at an angle which is indicated over the scalar printout. Then the diffractometer was set to scan through the X-ray peak. The total counts detected during the scan were integrated into a scalar. At the end of the scan the integrated counts were printed out. The scalar was reset to zero and another scan was made. The scan was generally repeated five times. In the two temperature technique a set of intensity measurements was made at room temperature then another set was made at either liquid nitrogen or helium temperature.

7-12-76
 00 00 00 00 00
 00

1000 1000 00
 400
 100000 100000
 000000 000000 000000 000000 000000 000000 000000

200
 40 100 50 100
 000011 000013 307107 307155 310708 310365 309741

300
 68 100 85 100
 000200 000290 000000 000000 013402 013500 013522 013490 013120

100
 20 100 30 100
 000003 000557 032239 032254 032500 032222 032053 000544

LIO N TEMP

400
 92 100 120 100
 000017 000482 057790 057809 057967 058130 057845

300
 70 100 85 100
 000277 000282 014270 014704 014775 014839 014875

200
 32 100 50 100
 000390 000313 321040 322700 322522 319801 321681

100
 10 100 20 100
 000012 000500 022300 022100 022303 022300 000000 022301 000100

SELECTED BIBLIOGRAPHY

- Anderson, O. L. (1963) J. Phys. Chem. Solids, 24, 909.
- Blackman, M. (1937) Proc. Cambridge Phil. Soc. 33, 381.
- Blackman, M. (1951) Proc. Phys. Soc. London, Ser. A, 64, 681.
- Blackman, M. (1955) Hdbk. der Physik, VII, 1, 325.
Berlin: Springer-Verlag.
- Bolsaitis, P. & Skolnick, L. (1968) Trans. A.I.M.E. 242, 215.
- Bolsaitis, P. & Chiarodo, R. (1971) to be published.
- Bolsaitis, P. (1970) Private communication.
- Born, M. (1942) Rep. Prog. Phys. (Phys. Soc.) 9, 249.
- Born, M. & Huang, K. (1955) Dynamical Theory of Crystal Lattices. Oxford: The Clarendon Press.
- Bowen, D. B. (1954) Acta. Met., 2, 573.
- Chiarodo, R. (1971) PhD. Thesis, University of Maryland, Engineering Materials Group.
- Chipman, D. R. (1956) J. Appl. Phys. 27, 7, 739.
- Chipman, D. R. & Paskin, A. (1959 A) J. Appl. Phys., 30, 1922.
- Chipman, D. R. & Paskin, A. (1959 B) J. Appl. Phys., 30, 1998.
- Cromer, D. T. (1965) Acta. Cryst., 18, 17.
- Cullen, W. (1970) Private communication.
- Cullity, D. B. (1956) Elements of X-ray Diffraction, Reading: Addison Wesley.
- Daniels, W. B. & Smith C. S. (1958) Phys. Rev., 111, 713.
- Dauben, C. H. & Tempelton, D. H., (1955), Acta Cryst., 8, 841.
- Debye, P. (1914) Ann. d. Physik, 43, 49.

- Doyle, P. A. & Turner, P. S. (1968) *Acta Cryst.*, A24, 390.
- Dozier, C. M., Gilfrich, J. V. & Birks, L. S. (1967) *Applied Optics*, 6, 2136.
- Einstein, A. (1911) *Ann. Phys. Lpz.*, 35, 679.
- Feldman, J. L. & Horton, G. K. (1967) *Proc. Phys. Soc.*, 92, 227.
- Flinn, P. A. (1960) *J. Phys. Chem. Solids*, 15, 189.
- Flinn, P. A., McManus, G. M. & Rayne, J. A. (1961) *Phys. Rev.*, 123, 3, 809.
- Frohn Meyer, G. & Glocker, R. (1953) *Acta Cryst.*, 6, 19.
- Fukuda, Y. (1952) *Tohoku Univ. Sci. Rpt.*, 1st series, 36, 273.
- Gehlen, D.C. & Cohen, J.B. (1969) *J. Appl. Phys.*, 40, 13, 5193.
- General Electric (1959) X-ray wave lengths for spectrometer, Cat. No. A4961DA.
- Guinier, A. (1963) *X-ray Diffraction*, San Francisco: W. H. Freeman and Company.
- Herbstein, F. H. (1961) *Adv. in Phys.* 10, 313.
- Huang, K. (1947) *Proc. Roy. Soc. London*, A190, 102.
- Hume-Rothery, W. & Powell, H. M. (1935) *Z. Kristallog.*, 91, 23.
- International Tables for X-ray Crystallography (1955) Birmingham, England: The Kynoch Press, Vol. III p. 210.
- James, R. W. (1948) *The Optical Principles of the Diffraction of X-rays*, London: G. Bell and Sons Ltd.
- Johansson, C. H. & Linde, J. O. (1936) *Ann. Phys. Lpz.* 5, 25, 1.
- Kittel, C. (1953) *Introduction to Solid State Physics*, New York: John Wiley & Sons, Inc.
- Kittel, C. (1967) *Introduction to Solid State Physics*, New York: John Wiley & Sons, Inc.
- Krivoglaz, M. A. (1969) *Theory of X-ray and Thermal Neutron Scattering by Real Crystals*, New York: Plenum Press.

- Leibfried, G. (1955) Hdbk. der Physik, VII, 1, 104.
Berlin: Springer-Verlag.
- Lindeman, R. (1910) Zeit. f. Physik, 11, 609.
- Lipson, H. (1950) Progress in Metal Physics II, London:
Butterworths Scientific Publications, 47.
- Lonsdale, K. (1948) Acta. Cryst., 1, 142.
- Maradudin, A. A., & Flinn, P. A. (1963) Phys. Rev., 129,
6, 2529.
- Maradudin, A. A., Montroll E. W. & Weiss, G. H., (1963)
Solid State Physics, Suppl. 3, New York: Academic
Press.
- Nix, F. C. & McNair D., (1941) Phys. Rev., 60, 320.
- Owen E. A. & O'D Roberts, E. A. (1945) J. Inst. Metals,
71, 213.
- Owen, E. A. & Evans, E. W. (1967) Brit. J. Appl. Phys.,
18, 1559.
- Owen, E. A. & Williams, R. W. (1947) Proc. Roy. Soc.
(London), A188, No 1015, 509.
- Passaglia, E. & Love, W. F. (1955) Phys. Rev., 98, 4,
1006.
- Rayne, J. A. (1957) Phys. Rev., 108, 3, 649.
- Sanderson, R. T. (1960) Chemical Periodicity, New York:
Reinhold Publ. Co., 25.
- Schwartz, L. H. & Cohen, J. B. (1965) J. Appl. Phys.,
36, 2, 598.
- Schwartz, L. H., Morrison, L. A. & Cohen, J. B. (1964)
Adv. of X-ray Analysis, 7, 281, New York: Plenum
Press, Inc.
- Skelton, E. F. & Katz, J. L. (1969) Acta Cryst., A25,
319.
- Sparks, C. J. & Borie, B. (1966) Local Arrangements
Studied by X-ray Diffraction, New York. Gordon and
Breach Science Publishers.
- Synecek, V., Simerska, M. & Chessin, H. (1969) Acta
Metallurgica, 3, 687.

- Waller, I. (1923) Zeit, f. Physik. 17, 398.
- Warren, B. E. (1969) X-ray Diffraction, Reading: Addison-Wesley Publishing Co.
- Webb, W. W. (1962) J. Appl. Phys., 33, 13, 3546.
- Wigner, E. & Seitz, F. (1934) Phys. Rev., 46, 509.
- Ziman, J. M. (1964) Principles of the Theory of Solids, Cambridge: The University Press.
- Zaviagina, A. P. & Inveronova, V. I. (1960) Fiz. Tverd. Tela., 2, 118.

VITA

Name: Charles Matthew Gilmore.

Permanent address: 6217 Springhill Court
Greenbelt, Maryland 20770.

Degree and date to be conferred: Ph.D., 1971.

Date of birth: November 14, 1941.

Place of birth: Erie, Pennsylvania.

Secondary education: McDowell High School, 1959.

Collegiate institutions attended	Dates	Degree	Date of Degree
Pennsylvania State University	1959-63	B.S.	June 1963
Pennsylvania State University	1963-64	M.S.	Dec. 1964
University of Maryland	1965-71	Ph.D.	Jan. 1971

Major: Engineering Materials.
Minors: Mathematics, Physics.

Publications: Machlin, I. & Gilmore, C.M. (1966)
Metal Progress, 70, 3, 101.
Gilmore, C.M. & Wang, F.E. (1967)
Acta Cryst., 23, 177.
Murr, L., Smith, P.J. & Gilmore, C.M. (1967)
Phil. Mag., 17, 145, 8.

Positions held: Research Physicist
U.S. Naval Research Laboratory
Washington, D. C.
Materials Engineer
U.S. Bureau of Naval Weapons
(and U.S. Naval Ordnance Laboratory)
Washington, D. C.